

FIG. 1.1. Illustration of graph-structured signals. Left: sensor network, right: Brain functional network [25]

40 which can incorporate graph structure of signals and can be implemented with simplicity and  
 41 efficiency.

42 **1.1. Motivation.** In last few decades, owing to its effectiveness on characterizing local dis-  
 43 continuities in a multi-scale manner, wavelet transform [11, 22] has been one fundamental tool in  
 44 classic signal processing. With the prevalence of sparse approximation/representation related theo-  
 45 ries and algorithms, wavelet tight frame based redundant transforms also see their wide adoptions in  
 46 many applications. For example, translational-invariant wavelet transform [8], and spline framelet  
 47 transform [12, 29]. There are several properties of wavelet/framelet transform that make it very  
 48 appealing to signal processing, including

- 49 (i) Localized analysis of signals in time domain by only employing operators defined on the  
 50 neighborhood of each point, which leads to effective characterizing of local discontinuities.
- 51 (ii) Multi-scale analysis of signals that enables the decomposition of a signal into a coarse  
 52 channel that encodes the smooth components of the signal and multiple channels that  
 53 encode the discontinuity details of the signal in multiple scales.
- 54 (iii) The *perfect reconstruction property* that enables the exact forward and backward process  
 55 of a signal and its transform coefficients
- 56 (iv) The simple and efficient cascade algorithms for signal decomposition and reconstruction.

57 A wavelet/framelet transform for signals defined on general graph is certainly of great interest to  
 58 many applications that involve graph-structured signals. However, owing to the irregular structure  
 59 of general graph, it is a challenging task to generalize discrete wavelet/framelet transform from  
 60 equi-spaced grid to general graph, while keeping all desired properties of classic wavelet/framelet  
 61 transforms listed above.

62 In recent years, there has been an enduring effort to generalize wavelet-type transform from  
 63 equispaced Euclidean grids to general graphs. Similar to the development of classic wavelet trans-  
 64 form, the construction of wavelet-type transform can be roughly classified into vertex domain based  
 65 approach [10, 36, 23, 37, 16, 26, 5, 6] and spectral domain based approach [9, 21, 17, 19, 32, 33, 35,  
 66 39, 13]. The majority of vertex domain based approaches are based on the construction of a tree  
 67 graph that abstracts the graph with certain properties, e.g., the  $k$ -hop connectivity between the  
 68 vertices. Such tree graphs are in parallel to the tree structure of multi-resolution analysis (MRA) in  
 69 equispaced grids, and thus classic MRA-based wavelet transforms can be directly defined from tree  
 70 graphs, which approximate the given graphs. Nevertheless, constructing a tree graph that keeps  
 71 most information of a given general graph is a very challenging optimization problem. Often, a tree

72 graph based abstraction of a general graph can lead to undesired loss of important information.  
 73 For instance, the shortest path distance of the graph for analyzing computer network traffic.

74 The spectral domain based approach is based on spectral structure of a graph, which is repre-  
 75 sented by the eigenvalues and eigenvectors of the graph Laplacian defined on the adjacent matrix  
 76 of the graph. These eigenfunctions provide a spectral decomposition for signals on graph similar  
 77 to discrete Fourier transform (DFT) for classic signals. As the convolution, one key operation in  
 78 wavelet transform, can be expressed as diagonal multiplication in spectral domain, the general-  
 79 ization of classic wavelet transform can be naturally done in spectral domain. Nevertheless, the  
 80 construction of wavelet transform in spectral domain also has its own issues. One is the localiza-  
 81 tion of the transform in vertex domain. In contrast to vertex domain based construction, it is quite  
 82 challenging to design transforms in spectral domain that running local operations in vertex domain,  
 83 while keeping perfect reconstruction property. Indeed, most existing spectral domain based wavelet  
 84 transforms either do not have good localization in vertex domain or do not have perfect recon-  
 85 struction property. Also, existing spectral domain based wavelet transforms do not provide many  
 86 choices, as they are specifically derived for certain examples of wavelet transform in equi-spaced  
 87 grids.

88 **1.2. Aim and the approach.** This paper aims at generalizing classic discrete framelet trans-  
 89 form to signals defined on undirected graphs. The discrete framelet transform proposed in this paper  
 90 will leverage the intuition from classic framelet transform in Euclidean spaces such that it not only  
 91 replicates classic framelet transform on equispaced grids, but also keeps those desired properties  
 92 during the generalization, including multi-scale analysis, and perfect reconstruction property.

93 We take a new approach to construct discrete framelet transform for signals on undirected  
 94 graphs. Different from those tree graph based constructions, the proposed approach is directly  
 95 defined on the original graph without tree-structured abstraction. Different from those constructions  
 96 in spectral domain, the proposed approach views the fundamental analogy between signal processing  
 97 on equispaced grids and undirected graphs is on the definition of the shift (translation) operator,  
 98 i.e., how the information propagates from one vertex to its neighbors. By taking the shift operator  
 99 as the fundamental building block, it is very natural to introduce the discrete convolution on graph,  
 100 which greatly facilitates the construction of framelet transform with two important properties: the  
 101 localization in vertex domain and the perfect reconstruction property. Discrete Fourier transform  
 102 is defined as the eigenvectors of the induced translation operator, which remains consistent with  
 103 the existing spectral approach. Together with the introduction of up/down-sampling in spectral  
 104 domain, the proposed approach generalizes the classic framelet transform from equispaced grids to  
 105 undirected graphs.

106 The construction focuses on the design of undecimal framelet transform. Undecimal trans-  
 107 form is also often called translation-invariant transform in signal processing. For a signal defined  
 108 on an equispaced grid, owing to the inclusion of down-sampling operation, the standard decimal  
 109 wavelet/framelet transform is not invariant to the shifts of the signal over the grid. That is, the  
 110 wavelet/framelet coefficients of a signal after a shift are not the same as (up to a shift) its original  
 111 counterpart. The sensitivity of framelet coefficients with respect to shifts is not desirable in many  
 112 applications. In practice, undecimal wavelet/frame transforms are often more preferred than its  
 113 decimal counterpart in signal/image recovery. For example, translation-invariant wavelet transform  
 114 for signal/image denoising [8], undecimal spline framelet transform for many image recovery tasks  
 115 including image inpainting, deconvolution, and volume data reconstruction [2, 38, 3, 4, 20].

116 The paper is organized as follows. We first present the definition and algorithm of multi-scale  
 117 un-decimal framelet transform for signals on undirected graphs. Then, a sufficient condition for

118 guaranteeing the perfect reconstruction property of multi-scale framelet transform is established for  
 119 both bi-frames and tight frames. Indeed, the proposed sufficient condition is closely related to the  
 120 Mixed Extension Principle (MEP) for classic wavelet bi-frames and the Unitary Extension Principle  
 121 (UEP) for classic wavelet tight frames. As a result, we have a painless construction of undecimal  
 122 multi-level framelet transform for signals defined on graphs. For example, the filter banks associated  
 123 with spline wavelet tight frames [12, 29] can be directly called for defining undecimal multi-level  
 124 tight framelet transform on graphs. In summary, this paper present an approach to construct  
 125 undecimal framelet transform for signals on graphs that leverages the properties of classic framelet  
 126 transform for signals defined on equispaced grids. In the remaining of the paper, Section 2 gave  
 127 a brief review on related works in existing literature. Section 3 presented related mathematical  
 128 preliminaries, including multi-level discrete framelet transform in Euclidean spaces and some basic  
 129 concepts in graph theory. In Section 4, we gave the notion of shift operator and other fundamental  
 130 operators in wavelet transform. Based on these key operators, we defined the multi-level framelet  
 131 transform on undirected graph and discussed its perfect reconstruction property in Section 5. In  
 132 Section 6, we demonstrated some examples of proposed discrete framelet transform on irregular  
 133 graph. Finally, in Section 7, we concluded the paper.

134 **2. Related work.** In recent years, there have been an enduring research effort on defining  
 135 and constructing wavelet-type transforms for signals on graph. In this section, we only give a brief  
 136 review on those most related works, which either define and construct wavelet related transform in  
 137 vertex domain or graph spectral domain.

138 The approach in vertex domain utilizes spatial features of graph to exploit local information  
 139 in the neighborhood of each vertex, e.g. vertex connectivities and edge weights. Representative  
 140 works include graph wavelets [10], lifting wavelets on graph [36, 23], and tree based construction of  
 141 wavelet transforms [16, 5, 6, 27, 28]. Crovella and Kolaczyk [10] proposed localized graph wavelet  
 142 transform for signals on unweighted graph, in which the wavelet function at scale  $j$  centered around  
 143 each vertex is strictly supported in a  $j$ -hop disk, i.e. set of vertices whose shortest path distance  
 144 from the center is less than or equal to  $j$ . Across different scales, the support of wavelet function  
 145 varies with  $j$ , which makes the transform able to examine local differences of a set of measurements  
 146 in a multi-scale fashion. However, the transform defined in [10] is not invertible in general. In the  
 147 lifting wavelet transform for graph proposed in ([36, 23]), at each scale, the vertex set is partitioned  
 148 into sets of even and odd vertices. Then similar to the standard lifting scheme, the coefficient on an  
 149 odd (or even) vertex is computed using its own signal value and signal values on its neighboring even  
 150 (or odd) vertices. In the process of even-odd splitting of vertices, partial graph information of each  
 151 vertex is lost, owing to the irregular structure of general graphs. For example, the adjacent vertices  
 152 are artificially allocated to the same parity, and thus partial information of the neighborhood of  
 153 any vertex is discarded in such a process.

154 In [16, 6], the graph, either directed or undirected, is clustered by some general-purpose clus-  
 155 tering algorithm into hierarchical tree, which has the same topological structure as classic MRA  
 156 defined on equispaced grids. Thus, classic wavelet systems defined on equispaced grids can be  
 157 generalized to the tree in a straightforward way. Based on such a concept, various multi-scale  
 158 wavelet-like transforms have been proposed in the past. For example, Haar wavelet on tree [16],  
 159 and orthonormalized systems of tree polynomials [5, 6]. In [27, 28], an  $L$ -level tree (or general-  
 160 ized tree) is constructed based on the distances among data points, which essentially is a rooted  
 161  $L$ -partite graph. The decomposition operation is different from the classic one by adding an ad-  
 162 ditional re-ordering process on low-pass (approximation) coefficients at each level, which shortens  
 163 the path passing through the coefficient. As a result, the smoothness of low-pass coefficients is

164 improved and high-pass wavelet coefficients have better sparsity degree. Nevertheless, these tree  
 165 based construction schemes of wavelet transforms depend on the abstraction process that converts  
 166 a general graph into a graph with tree structure, which is difficult to have an optimal approach that  
 167 keeps most geometrical information of a general graph. Certain important information is likely to  
 168 be discarded in such an abstraction, e.g. the connectivity among adjacent vertices.

169 A prominent approach of constructing wavelet-type transform on graph is done in graph spec-  
 170 tral domain, i.e., the generalized discrete Fourier transform on graph. Representative works of such  
 171 an approach include diffusion wavelets [9, 21, 1] and Laplacian-based transforms [17, 18, 19, 39, 13,  
 172 24, 31]. In these works, basic operators and multi-scale structure involved in wavelet transform are  
 173 defined using spectral features, including the eigenvalues and eigenvectors of graph Laplacian ma-  
 174 trix derived from the adjacency matrix of a graph. Coifman and Maggioni [9] introduced diffusion  
 175 wavelets for multi-scale representation of signals on manifolds and graphs, in which the dilation  
 176 operator involved in classic wavelet transform is replaced by a diffusion operator. At each scale, the  
 177 dyadic power of diffusion operator is first applied on basis elements and the resulted functions are  
 178 then down-sampled via a localized orthonormalization scheme to produce an orthonormal basis for  
 179 the next coarse level. Then, the wavelet functions are constructed by collecting locally orthogonal-  
 180 izing atoms spanning the difference between two consecutive levels, which leads to an orthonormal  
 181 wavelet-type transform on graph. It is further extended to bi-orthogonal diffusion wavelets [21] and  
 182 diffusion wavelet packets in [1] for manifolds and graphs. However, it is indicated in [17] that the  
 183 orthogonalization procedure in the construction of diffusion wavelets is quite complicated, and it  
 184 obscures the relationship between diffusion operator and resulting wavelets.

185 Based on graph Laplacian [7], another type of spectral graph wavelet transforms is introduced in  
 186 [17], which defines the shift, discrete convolution and dilation operators all in graph spectral domain,  
 187 which is in parallel to the Fourier transform based expression of these operations in equispaced grids.  
 188 The operators related to the scaling and wavelet functions are then defined using the generalized  
 189 convolution, spectral scaling kernel and wavelet kernels dilated at different scales. Many consequent  
 190 works follow such an approach, and the main difference lies in which spectral kernels are used to  
 191 generate wavelet systems. For example, in [18, 19], tight wavelet frames are constructed by using  
 192 Meyer-like wavelet and scaling kernels. Based on definition of the translation and warping in the  
 193 graph spectral domain, spectral kernels are adapted in [39] to the distribution of graph Laplacian  
 194 eigenvalues to yield spectrum-adapted tight graph wavelet frames. Another wavelet frame transform  
 195 on graph is introduced in [13], which considered the construction of wavelet tight frames on both  
 196 manifolds and graphs. In [13], the wavelet functions on manifold are generated from a refinable  
 197 function and a filter bank that includes both refinement masks and wavelet masks. The filter  
 198 bank is then used as the spectral kernels for generating systems on graph. It is shown in [13] that  
 199 tight frame property of proposed quasi-affine systems (undecimal system) on manifolds, as well  
 200 as associated discrete multi-level systems on graphs, is guaranteed by one of conditions in *unitary*  
 201 *extension principle* [29, 12] for classic MRA-based wavelet tight frame in Euclidean space.

202 In comparison to vertex domain based transforms, graph Laplacian based wavelet-type trans-  
 203 forms usually do not include down/up-sampling process, **as how to meaningfully down-sample a**  
 204 **graph is not clear in general**. For specific types of graph, particularly bipartite graph, the vertices  
 205 can be divided into two dis-joint subsets such that there is no edge inside each subset. Such property  
 206 allows a down-sampling process in parallel to its counterpart in equi-spaced grids. By consequen-  
 207 tially decomposing a general graph into bi-partite subgraphs, a class of two-channel critically sam-  
 208 pled orthonormal wavelet transforms are proposed in [24]. **In [31], the down/up-sampling process is**  
 209 **designed in the spectral domain via spectrum folding of frequencies. With such down/up-sampling**

210 approach, the two-channel graph Laplacian based (bi-)orthogonal wavelet transform is constructed  
 211 in [31].

212 Furthermore, since the atoms associated with the graph Laplacian based transforms are eigen-  
 213 vectors of the graph Laplacian, they are usually not localized in vertex domain. For computational  
 214 efficiency, sometimes such transforms are approximated using Chebyshev polynomials of graph  
 215 Laplacian (e.g. [17, 13]). When adopting Chebyshev polynomials approximation based computa-  
 216 tional scheme, the perfect reconstruction property of the original wavelet transform does not hold  
 217 true anymore. The computation using Chebyshev polynomials indeed is parallel to the recent work  
 218 on digital signal processing that defines convolution operations directly from the adjacency matrix.

219 The recent work on digital signal processing on graph ([32, 33, 34, 35]) is very related to wavelet-  
 220 type transform on graph. The basic operations often seen in digital signal processing, including  
 221 shift operator, discrete convolution, and frequency response, are also the fundamental operations  
 222 involved in wavelet-type transforms. In [32, 33, 34, 35], the shift operator serves as basic building  
 223 block to define convolution, Fourier transform, frequency responses and so on. The shift operator in  
 224 these works is defined as the adjacency matrix of the graph, regardless directed or undirected graph.  
 225 Such definition of shift operator on undirected graphs has its issues, as it can not replicate its classic  
 226 counterpart on 1D equispaced grids with periodic boundary extension, i.e., a cyclic permutation  
 227 matrix. In addition, some other ingredients and properties involved in wavelet transform are not  
 228 discussed in these works, e.g. down/up sampling operations and perfect reconstruction property.

229 **3. Preliminaries.** We first give an introduction to the notations used in this paper. Through  
 230 this paper, we use  $\mathbb{Z}, \mathbb{Z}^+, \mathbb{R}, \mathbb{C}$  to denote the set of integers, positive integers, real-valued numbers  
 231 and complex-valued numbers, respectively. The cardinality of a finite set  $\Xi$  is denoted by  $|\Xi|$ . For  
 232 any  $M \in \mathbb{Z}^+$ , define  $\mathbb{Z}_M := [-(M-1), M-1] \cap \mathbb{Z}$ . For any  $x \in \mathbb{C}$ , let  $x^*$  denote its complex  
 233 conjugate. We denote the linear space of all sequences by  $\ell(\mathbb{Z})$ , and the linear space of all sequences  
 234 with finite non-zero elements by  $\ell_0(\mathbb{Z})$ . For any sequence  $f \in \ell(\mathbb{Z})$ , its  $k$ -th element is denoted by  
 235  $f[k]$ . For a matrix  $A \in \mathbb{C}^{M \times N}$ , let  $A_j$  denote its  $j$ -th column, and  $A_{k,j}$  the entry at its  $k$ -th row and  
 236  $j$ -th column. The conjugate transpose of a matrix  $A$  is denoted by  $A^*$ , and its inverse is denoted  
 237 by  $A^{-1}$  if exists. Let  $I_N$  denote the  $N \times N$  identity matrix. For matrix concatenation, semi-colons  
 238 are used for adding elements in columns and commas are used for adding elements in rows.

**3.1. MRA-based Wavelet tight (bi) frames.** In this section, we give a brief introduction to  
 multi-scale (or multi-level) discrete framelet transform for signals defined on equispaced Euclidean  
 grids. Consider a Hilbert space  $H$  with inner product  $\langle \cdot, \cdot \rangle$ . A sequence  $\{v_n\}_{n \in \mathbb{Z}} \subset H$  is called a  
*frame* if there exist two positive constant  $A, B$  such that

$$A\|f\|^2 \leq \sum_{n \in \mathbb{Z}} |\langle f, v_n \rangle|^2 \leq B\|f\|^2, \quad \forall f \in H.$$

239 The sequence  $\{\tilde{v}_n\}_{n \in \mathbb{Z}} \subset H$  is called its *dual frame* if

$$240 \quad (3.1) \quad f = \sum_{n \in \mathbb{Z}} \langle f, v_n \rangle \tilde{v}_n = \sum_{n \in \mathbb{Z}} \langle f, \tilde{v}_n \rangle v_n, \quad \forall f \in H.$$

241 A frame  $\{v_n\}_{n \in \mathbb{Z}}$  is called *tight frame* when  $A = B = 1$ . For a tight frame, one of its dual frames  
 242 is the tight frame itself. A frame  $\{v_n\}_{n \in \mathbb{Z}}$  and its dual  $\{\tilde{v}_n\}_{n \in \mathbb{Z}}$  are called *bi-frames* for  $H$ .

Multi-scale discrete framelet transform for signals defined on equi-spaced grids is derived from  
 MRA-based wavelet frames for  $L_2(\mathbb{R})$ . Consider a refinable function  $\phi \in L_2(\mathbb{R})$  with  $\hat{\phi}(0) = 1$  that

satisfies

$$\phi(k) = 2 \sum_{k \in \mathbb{Z}} h_0[k] \phi(2x - k),$$

for some finite sequence  $h_0 \in \ell_0(\mathbb{Z})$ , the so-called refinement mask of  $\phi$ . The function  $\phi$  admits a multi-resolution analysis (MRA) of  $L_2(\mathbb{R})$ , if the sequence of subspaces  $\{V_n\}_{n \in \mathbb{Z}} \subset L(\mathbb{R})$  defined by

$$V_n = \overline{\text{span}\{2^{\frac{n}{2}} \phi(2^n - k)\}_{k \in \mathbb{Z}}}$$

satisfies

$$(1) V_n \subset V_{n+1}, \quad n \in \mathbb{Z}, \quad (2) \overline{\cup_n V_n} = L_2(\mathbb{R}), \quad (3) \cap_n V_n = \{0\}.$$

Define a set of framelets  $\Psi = \{\psi_j\}_{j=1}^r$  as

$$\psi_j(\cdot) = 2 \sum_{k \in \mathbb{Z}} h_j[k] \phi(2 \cdot - k), \quad 1 \leq j \leq r.$$

243 Then, the UEP [29, 12] says that the corresponding wavelet (affine) system defined by

$$244 \quad (3.2) \quad X(\Psi) = \{2^{n/2} \psi_j(2^n \cdot - k)\}_{1 \leq j \leq r, n, k \in \mathbb{Z}}.$$

245 will form a tight frame for  $L_2(\mathbb{R})$ , if the masks  $\{h_0, h_1, \dots, h_r\}$  satisfy

$$246 \quad (3.3) \quad \sum_{j=0}^r \sum_{n \in \Omega_k} (h_j[n])^* h_j[n+m] = 2^{-1} \delta_{m,0}$$

247 for all  $m \in \mathbb{Z}$ ,  $k \in \mathbb{Z}/2\mathbb{Z}$ , where  $\Omega_k = (2\mathbb{Z} + k) \cap \text{supp}(h_0)$ . The set of masks  $H = \{h_0, h_1, \dots, h_r\}$   
 248 is often called *wavelet filter bank*.

For wavelet bi-frames, suppose that we have two refinable functions  $\phi, \tilde{\phi}$  with refinable masks  $h_0, \tilde{h}_0$ , and each of which admits an MRA for  $L_2(\mathbb{R})$ . Define two sets of framelets  $\Psi = \{\psi_j\}_{j=1}^r, \tilde{\Psi} = \{\tilde{\psi}_j\}_{j=1}^r$  as follows,

$$\psi_j(\cdot) = 2 \sum_{k \in \mathbb{Z}} h_j[k] \phi(2 \cdot - k); \quad \tilde{\psi}_j(\cdot) = 2 \sum_{k \in \mathbb{Z}} \tilde{h}_j[k] \tilde{\phi}(2 \cdot - k),$$

for  $j = 1, \dots, r$ . Then, the MEP [15] shows that under very mild conditions, two wavelet (affine) systems given by

$$X(\Psi) = \{2^{n/2} \psi_j(2^n \cdot - k)\}_{1 \leq j \leq r, n, k \in \mathbb{Z}}; \quad X(\tilde{\Psi}) = \{2^{n/2} \tilde{\psi}_j(2^n \cdot - k)\}_{1 \leq j \leq r, n, k \in \mathbb{Z}}.$$

249 form bi-frames for  $L_2(\mathbb{R})$ , if the two mask sets  $\{h_j\}_{j=0}^r$  and  $\{\tilde{h}_j\}_{j=0}^r$  satisfy

$$250 \quad (3.4) \quad \sum_{j=0}^r \sum_{n \in \Omega_k} (h_j[n])^* \tilde{h}_j[n+m] = 2^{-1} \delta_{m,0}.$$

In the context of signal processing, it is often more preferred to use a shift-invariant system. Recall that a system  $X$  is called shift-invariant if for any  $g \in X$  and any  $k \in \mathbb{Z}$ , we have  $g(\cdot - k) \in X$ . To have such a shift-invariant property, the wavelet system  $X(\Psi)$  needs to be over-sampled for the level  $n < 0$ , which is called a quasi-affine system. More specifically, consider a wavelet system

$X(\Psi) = \{2^{n/2}\psi_j(2^n \cdot -k)\}_{1 \leq j \leq r; n, k \in \mathbb{Z}}$ , its quasi-affine version from level 0, denoted by  $X^q(\Psi) = \{\psi_{j,n,k}^q\}_{1 \leq j \leq r, n, k \in \mathbb{Z}}$ , is defined by

$$\psi_{j,n,k}^q = \begin{cases} 2^{n/2}\psi_j(2^n \cdot -k), & n \geq 0, \\ 2^n\psi_j(2^n \cdot -2^n k), & n < 0. \end{cases}$$

251 If  $X(\Psi)$  is a tight wavelet frame for  $L_2(\mathbb{R})$  obtained from the UEP, the quasi-affine system  $X^q(\Psi)$   
 252 defined above also forms a tight frame for  $L_2(\mathbb{R})$ . More details regarding quasi-affine systems and  
 253 tight frames can be found in [29].

**3.2. Multi-level discrete framelet transform.** Once an MRA-based wavelet bi-frames or tight frames for  $L_2(\mathbb{R})$  are constructed via the construction of the masks satisfying the MEP or UEP, we have in hand a filter bank (the set of masks) based efficient numerical implementation of multi-level decomposition and reconstruction for discrete signals. For simplicity, we only present the discrete framelet transform with finite supported filter bank on the sequence space  $\ell(\mathbb{Z})$ , it can be easily generalized to the finite signal space  $\mathbb{C}^N$  by periodic boundary extension. Discrete framelet transform has two parts: framelet decomposition and framelet reconstruction, and they are built on three basic operations. One is discrete convolution:

$$(f \otimes h)[m] = \sum_{k \in \text{supp}(h)} h[k]f[m-k], \quad \text{for any } f \in \ell(\mathbb{Z}),$$

254 where  $h$  denotes a filter in  $\ell_0(\mathbb{Z})$ . One is down-sampling operator:

$$255 \quad (3.5) \quad (f \downarrow_2)[k] = f[2k],$$

256 and the other is up-sampling operator:

$$257 \quad (3.6) \quad (f \uparrow_2)[k] = \begin{cases} f[\frac{k}{2}], & \text{if } \frac{k}{2} \in \mathbb{Z}, \\ 0, & \text{otherwise.} \end{cases}$$

258 There are two basic operators involved in framelet transform. Given a filter  $h \in \ell_0(\mathbb{Z})$ , one is the  
 259 transit operator  $W_h : \ell(\mathbb{Z}) \rightarrow \ell(\mathbb{Z})$  defined by

$$260 \quad (3.7) \quad W_h f = (f \otimes h^*[\cdot]) \downarrow_2.$$

261 The other is subdivision operator:  $W_h^* : \ell(\mathbb{Z}) \rightarrow \ell(\mathbb{Z})$  defined by

$$262 \quad (3.8) \quad W_h^* c = (c \uparrow_2) \otimes h.$$

263 Let  $H = \{h_0, h_1, \dots, h_r\} \subset \ell_0(\mathbb{Z})$  denote the filter bank that defines wavelet frame  $X(\Psi)$ , and  
 264  $\tilde{H} = \{\tilde{h}_0, \tilde{h}_1, \dots, \tilde{h}_r\} \in \ell_0(\mathbb{Z})$  the filter bank that defines the dual frame  $X(\tilde{\Psi})$ . In the case of  
 265 wavelet tight frame,  $H = \tilde{H}$ .

266 A one-level framelet transform comprises two operators: decomposition and reconstruction.  
 267 The decomposition operator  $W_H : \ell(\mathbb{Z}) \rightarrow \ell(\mathbb{Z})^{1 \times (r+1)}$  is defined as: for any  $f \in \ell(\mathbb{Z})$ ,

$$268 \quad (3.9) \quad W_H f := (W_{h_0} f, W_{h_1} f, \dots, W_{h_r} f).$$

269 The reconstruction operator  $W_{\tilde{H}}^* : \ell(\mathbb{Z})^{1 \times (r+1)} \rightarrow \ell(\mathbb{Z})$  is defined by:

$$270 \quad (3.10) \quad W_{\tilde{H}}^* c = W_{\tilde{h}_0}^* c_0 + W_{\tilde{h}_1}^* c_1 + \dots + W_{\tilde{h}_r}^* c_r.$$

Then, *perfect reconstruction property* of bi-frames or tight frames leads to

$$W_H^* W_H = I \quad (\text{bi-frames}), \quad \text{and} \quad W_H^* W_H = I \quad (\text{tight frames}),$$

where  $I$  is identity operator.

One motivation of discrete framelet transform is for effectively extracting multi-scale structures of input signals, which requires the so-called multi-level discrete framelet transform. Multi-level discrete framelet transform is done by recursively performing one-level discrete framelet transform on only one selected sequence of framelet coefficients, which is called low-pass framelet coefficients generated from a low-pass filter (the refinement mask  $h_0$ ). The framelet coefficients and their associated filters in other sequences, which are not selected for further decomposition, are called high-pass framelet coefficients and high-pass filters (the wavelet masks  $\{h_1, \dots, h_r\}$ ). Let  $W_h$  and  $W_h^*$  denote the transit operator and subdivision operator defined as (3.7) and (3.8) respectively. Then, the decomposition procedure of an  $L$ -level framelet transform reads as follows. Initialize  $c_0^{(0)} = f$ . For  $\ell = 1, 2, \dots, L$ ,

$$(3.11) \quad c_j^{(\ell)} = W_{h_j} c_0^{(\ell-1)}, \quad \text{for } j = 0, 1, \dots, r.$$

The coefficients  $\{c_1^{(\ell)}, c_2^{(\ell)}, \dots, c_r^{(\ell)}\}_{\ell=1}^L \cup c_0^{(L)}$  are the  $L$ -level framelet coefficients of  $f$ . The reconstruction procedure reads as follows. For  $\ell = L - 1, \dots, 1, 0$ ,

$$(3.12) \quad c_0^{(\ell)} = \sum_{j=0}^r W_{h_j}^* c_j^{(\ell+1)}.$$

The signal  $f$  is then set as  $f = c_0^{(0)}$ . Recursively applying the perfect reconstruction property on each level, we also have the perfect reconstruction property for an  $L$ -level framelet transform. Interesting readers are referred to [14, 15, 38] for more details on MRA-based wavelet bi-frames, wavelet tight frames and discrete framelet transform.

The framelet transform introduced above is derived from the standard MRA-based wavelet tight frames or bi-frames for  $L^2(\mathbb{R})$ . For shift-invariant version of wavelet frames, we can define the so-called undecimal discrete framelet transform, which removes down-sampling operation in decomposition and up-sampling operation in reconstruction. Given a finite filter  $h$ , the transit operator  $W_h$  and the subdivision operator  $W_h^*$  are defined by

$$W_h f = f \otimes h^*(-\cdot), \quad \text{and} \quad W_h^* f = f \otimes h.$$

Recall that in decimal case, the coefficients at the coarser level have been down-sampled, while the coefficients at the coarser level in undecimal case have not been down-sampled. Notice that

$$(h \otimes (f \downarrow_{2^{\ell-1}})) = ((h \uparrow_{2^{\ell-1}}) \otimes f) \downarrow_{2^{\ell-1}},$$

which says the undecimal version of a down-sampled signal  $f \downarrow_{2^{\ell-1}}$  convolved with a filter  $h$  is indeed the original signal  $f$  convolved with the upsampled filter  $h \uparrow_{2^{\ell-1}}$ . Thus, at the  $\ell$ -th level, the transit operator  $W_h^{(\ell)}$  and subdivision operator  $(W_h^*)^{(\ell)}$  are given by

$$W_h^{(\ell)} f = (h^{(\ell)})^*(-\cdot) \otimes f, \quad \text{and} \quad (W_h^*)^{(\ell)} f = h^{(\ell)} \otimes f.$$

where  $h^{(\ell)} = h \uparrow_{2^{\ell-1}}$ .

**3.3. Basics on graph theory.** Recall that a graph  $G = (\mathcal{V}, E, \omega)$  comprises a set of vertices  $\mathcal{V} = \{v_p : p = 1, \dots, N\}$ , a set of edges  $E \subset \mathcal{V} \times \mathcal{V}$  and a weight function  $\omega : E \rightarrow \mathbb{R}^+$ . Its *adjacency matrix*  $S$  is an  $N \times N$  matrix defined by

$$S[p, q] = \begin{cases} \omega(v_p, v_q), & (v_p, v_q) \in E, \\ 0, & \text{otherwise,} \end{cases} \quad \text{for } 1 \leq p, q \leq N.$$

291 The degree matrix, denoted by  $D$ , is a diagonal matrix with its  $k$ -th diagonal element given by  
 292  $D[k, k] = \sum_{p=1}^N S[k, p]$ .

293 In this paper, we only consider signals defined on an undirected connected graph, which satisfies  
 294 the following properties:

- 295 • *Undirected*:  $(v_p, v_q) \in E$  if and only if  $(v_q, v_p) \in E$ , and  $\omega(v_p, v_q) = \omega(v_q, v_p)$  for any  
 296  $v_p, v_q \in V$ .
- 297 • *Connected*: there is a path between every pair of vertices in  $G$ .
- 298 • There exists no loop (an edge connecting a vertex to itself).

299 For a connected undirected graph, its adjacency matrix  $S$  satisfies the following properties:

- 300 1. The matrix  $S$  is symmetric.
- 301 2. The summation  $\sum_{j=1}^{N-1} S^j$  has no zero entries.
- 302 3. All diagonal entries of  $S$  are zero.

303 Then, a signal  $f = (f[1]; f[2]; \dots; f[N])$ , is a function defined on the vertices of the graph  $G =$   
 304  $(\mathcal{V}, E, \omega)$ , i.e.,  $f : \mathcal{V} \rightarrow \mathbb{C}^N$ .

**4. Key ingredients of discrete framelet transform on graph.** Before presenting undec-  
 imal framelet transform for signals on undirected graph, we first present in this section the gener-  
 alization of several basic concepts in signal processing, namely shift, convolution, down-sampling  
 and up-sampling, from equispaced Euclidean grids to undirected graph. Consider a signal  $f \in \mathbb{C}^N$   
 defined on the vertices of a graph  $G = \{\mathcal{V}, E, \omega\}$ . Let  $S \in \mathbb{C}^{N \times N}$  denote the adjacency matrix of  
 $G$ , and let  $D$  denote its degree matrix. Then, the matrix

$$D^{-\frac{1}{2}} S D^{-\frac{1}{2}}$$

305 is called the normalized adjacency matrix whose eigenvalues are inside  $[-1, 1]$  (see e.g. [7]). In the  
 306 next, we define the shift operator for undirected graph, which defines how a signal is translated  
 307 around the vertices of a graph. Such a shift operation is essential for defining discrete convolution.

308 **DEFINITION 4.1** (Graph shift operator). *Consider an undirected graph  $G$  with adjacency ma-*  
 309 *trix  $S \in \mathbb{R}^{N \times N}$ . A matrix  $\mathcal{T} \in \mathbb{C}^{N \times N}$  is called the unit shift operator of  $G$ , if  $\mathcal{T}$  is invertible,*  
 310 *normal and satisfies*

$$311 \quad (4.1) \quad D^{-\frac{1}{2}} S D^{-\frac{1}{2}} = \frac{1}{2}(\mathcal{T} + \mathcal{T}^*).$$

312  
 313 *The proposed definition for the shift operator is different from existing definitions of shift oper-*  
 314 *ator on graphs, which usually directly treats  $S$  as the shift operator. In Definition 4.1,  $\mathcal{T}$  is viewed*  
 315 *as the shift operator by 1-tap and its transpose  $\mathcal{T}^*$  is also a shift operator by 1 tap but toward the*  
 316 *opposite direction. Thus, the normalized adjacency matrix of an undirected graph is viewed the*  
 317 *average of shifting the graph by 1 tap on both directions. For any  $k \in \mathbb{Z}$ , the  $k$ -tap shift operator*  
 318 *is defined as  $\mathcal{T}^k$ . The graph shift operator in Definition 4.1 keeps many desired properties of its*  
 319 *counterpart for equispaced grids. To list some,*

- 320 • The invertibility of  $\mathcal{T}$  implies that shifting signal on graph will not remove information of
- 321 signal.
- 322 • The property  $\mathcal{T}^*\mathcal{T} = \mathcal{T}\mathcal{T}^*$  implies that shifting signals forward and shifting signal backward
- 323 should be commutative.
- 324 • The fact  $\mathcal{T}^{k_1}\mathcal{T}^{k_2} = \mathcal{T}^{k_1+k_2}$  implies that the shifts of the signal are accumulated.

325 By Definition 4.1, the shift operator is not unique. In the next, we present the construction  
 326 scheme of a special type of shift operators, the isometric shift operator that preserves the energy  
 327 of signals, i.e.  $\mathcal{T}$  is a unitary operator with  $\mathcal{T}^*\mathcal{T} = I$ . Isometry property is one basic property of  
 328 shift operator for equispaced grids, i.e., a signal energy is kept when being shifted around over the  
 329 graph. Isometry property of shift operator is certainly a desired property for signal processing. If  
 330 the shift operator is not isometric, after being shifted for many taps, the component of the signal  
 331 with respect to the largest eigenvalue will dominate the output, and all others disappear. Such a  
 332 behaviour certainly causes computational instability and inconsistency for multi-level analysis which  
 333 involves the concatenation of many convolutions.

CONSTRUCTION 1. [Isometric shift operator] Let  $S$  denote the adjacency matrix of an undirected graph  $G$ . Then  $D^{-\frac{1}{2}}SD^{-\frac{1}{2}}$  is symmetric, whose eigenvalues lie in  $[-1, 1]$ . Let  $U \in \mathbb{C}^{N \times N}$  denote the unitary matrix that diagonalizes the matrix  $S$ :

$$D^{-\frac{1}{2}}SD^{-\frac{1}{2}} = U^{-1}\Sigma U,$$

where  $\Sigma = \text{diag}(\underbrace{\mu[1], \dots, \mu[1]}_{m_1}, \underbrace{\mu[2], \dots, \mu[2]}_{m_2}, \dots, \underbrace{\mu[p], \dots, \mu[p]}_{m_p})$ . Define the shift operator  $\mathcal{T}$  as

$$\mathcal{T} = U^{-1}\Lambda U = U^{-1}\text{diag}(\lambda[1], \lambda[2], \dots, \lambda[N])U.$$

334 Then, the matrix  $\mathcal{T}$  is unitary and satisfies (4.1), if we set

$$335 \quad (4.2) \quad \lambda[k] = e^{i\theta_k}, \quad \text{with} \quad \cos(\theta_k) = \mu[j_k],$$

336 where for the same  $\mu[j_k]$ , the value  $\theta$  is assigned alternatively between  $\theta_k \in [0, \pi)$  and  $2\pi - \theta_k$ . That  
 337 is, for  $j = 1, 2, \dots, p$ ,

$$338 \quad (4.3) \quad \lambda[(\sum_{n=1}^{j-1} m_n) + k] := \mu[j] + i(-1)^{k-1} \sqrt{1 - (\mu[j])^2}, \quad \text{for} \quad k = 1, \dots, m_j.$$

339 The shift operator constructed in Construction 1 essentially takes the eigenvectors of adjacent matrix  
 340 as its eigenvectors and maps the eigenvalues of the adjacent matrix in  $[-1, 1]$  to the unit disk in  
 341 complex plane. Clearly, such a shift operator is unitary which preserves the energy when shifting the  
 342 signal around the graph. Such an energy-preserving property is similar to its counterpart in classic  
 343 equispaced grids, and does not attenuate any components of signals when being applied for multiple  
 344 times. The trade-off is that in general it is **not likely to have a sparse shift operator**  $\mathcal{T}$  even when  
 345 the adjacency matrix  $S$  is sparse.

346 With the availability of graph shift operator  $\mathcal{T}$ , we now define convolution operator for a finite  
 347 filter  $h = \{h[k]\}_{k \in \mathbb{Z}_M}$ . For simplicity, we restrict the filter size no larger than  $N$ .

348 DEFINITION 4.2 (Graph convolution operator). Consider a finite filter  $h = \{h[k]\}_{k \in \mathbb{Z}_M}$  and a  
 349 graph  $G$ . The convolution operator is defined as: for any signal  $f \in \mathbb{C}^N$ ,

$$350 \quad (4.4) \quad \mathcal{H}(h)f = \sum_{k \in \mathbb{Z}_M} h[k]\mathcal{T}^k f,$$

351 where  $\mathcal{T}$  denotes the shift operator defined in Definition 4.1.  
 352 By the basic property of matrix multiplication, we have

PROPOSITION 4.3 (Shift-invariance of convolution operator). *Let  $\mathcal{T}$  and  $\mathcal{H}(h)$  denote the shift operator and the convolution operator w.r.t. the filter  $h$ . Then, for any signal  $f \in \mathbb{C}^N$ ,*

$$\mathcal{H}(h)(\mathcal{T}^k f) = \mathcal{T}^k(\mathcal{H}(h)f).$$

353

354 In the next, we define another key block involved in framelet transform: dyadic down-sampling  
 355 and up-sampling operators for signals on graph  $G$ . Motivated by basic properties of their counter-  
 356 parts for equispaced grids, we proposed the following generalized down/up sampling operator such  
 357 that down-sampling an up-sampled signal does not lose the information of the signal.

358 DEFINITION 4.4 (Dyadic down(up)-sampling operator on graph). *The operator  $\Gamma_\downarrow \in \mathbb{C}^{\frac{N}{2} \times N}$   
 359 and its adjoint operator  $\Gamma_\uparrow = (\Gamma_\downarrow)^*$  are called the down-sampling operator and up-sampling operator,  
 360 provided that  $\Gamma_\downarrow \Gamma_\uparrow \in \mathbb{C}^{\frac{N}{2} \times \frac{N}{2}}$  is invertible.*

361 Clearly, the definition of down/up-sampling is not unique. In the next, we give a construction  
 362 scheme of down/up sampling operator satisfying the conditions imposed in Definition 4.4, which is  
 363 analogy to the reconstruction property of classical down-sampling operator on bandlimited signal.  
 364 More specifically, it is known that in 1D uniform grid, whether a signal can be perfectly reconstructed  
 365 from its samples depends on whether its frequencies fall into the interval determined by Shannon  
 366 sampling theorem. Thus, if a signal is bandlimited with the upper-half of its frequency spectrum  
 367 vanishes, the signal still can be exactly recovered from samples after being down-sampled. Before  
 368 introducing the down-sampling operator on graph that keeps such a property, we first introduce the  
 369 generalization of discrete Fourier transform from equispaced grids to graphs.

The definition of discrete Fourier transform on graph is then based on one fundamental property  
of classic discrete Fourier transform, i.e., the classic discrete Fourier transform is the matrix that  
diagonalizes the shift operator or equivalently the finite convolution operator on equispaced grids.  
Recall that by Definition 4.1,  $\mathcal{T}$  is an invertible normal matrix. Thus, there exists a unitary matrix  
 $V$  such that

$$\mathcal{T} = V^{-1} \Lambda V = V^{-1} \text{diag}(\lambda[1], \dots, \lambda[N]) V$$

370 where  $\{\lambda[k]\}_{k=1}^N$  are eigenvalues of  $\mathcal{T}$ , and they can be viewed as the generalized frequencies.

DEFINITION 4.5 (Discrete Fourier transform on graph (GDFT)). *For a graph  $G$ , its discrete  
Fourier transform on graph is the unitary matrix  $\mathcal{F} \in \mathbb{C}^{N \times M}$  that diagonalizes the shift operator  
 $\mathcal{T}$ :*

$$\mathcal{F} \mathcal{T} \mathcal{F}^{-1} = \text{diag}(\lambda[1], \lambda[2], \dots, \lambda[N]).$$

371

372 It can be seen that when we adopt the shift operator defined in Construction 1, the GDFT  $\mathcal{F}$  is  
 373 the same as the unitary matrix that diagonalizes the adjacency matrix.

374 PROPOSITION 4.6 (Convolution theorem). *Let  $\mathcal{H}$  and  $\mathcal{F}$  denote the convolution operator and  
 375 discrete Fourier transform defined in Definition 4.2 and 4.5 respectively. Then,  $\mathcal{F} \mathcal{H} \mathcal{F}^{-1}$  is a diag-  
 376 onal matrix.*

*Proof.* By the definition  $\mathcal{F}$  and  $\mathcal{H}$ , we have

$$\mathcal{H}(h) = \sum_{k \in \mathbb{Z}_M} h[k] \mathcal{T}^k = \sum_{k \in \mathbb{Z}_M} h[k] (\mathcal{F}^{-1} \Lambda \mathcal{F})^k = \mathcal{F}^{-1} \left( \sum_{k \in \mathbb{Z}_M} h[k] \Lambda^k \right) \mathcal{F}.$$

377 Since  $\sum_{k \in \mathbb{Z}_M} h[k] \Lambda^k$  is a diagonal matrix, we have  $\mathcal{F} \mathcal{H} \mathcal{F}^{-1}$  is a diagonal matrix.  $\square$

Recall that up-sampling and down-sampling on equispaced grids, expressed in vertex domain as (3.5) and (3.6), can also be expressed in frequency domain in terms of frequency folding operation. Let  $\widehat{\cdot}$  denote the classical discrete Fourier transform. Then, we have

$$(\widehat{f \downarrow_2})[k] = \frac{1}{2} \left( \widehat{f}[k] + \widehat{f}\left[k + \frac{N}{2}\right] \right), \quad \text{for } k = 1, \dots, \frac{N}{2},$$

378 where  $\widehat{f}[k]$  refers the frequency  $e^{i2\pi \frac{k-1}{N}}$ . In other words, down-sampling on equi-spaced grid is the  
 379 same as folding its frequencies by one half. To generalize it from equispaced grid to graph, one first  
 380 needs to assign the frequency magnitude to each eigenvalue of  $\mathcal{T}$ , so that the eigenvalues of  $\mathcal{T}$  can  
 381 be appropriately ordered to making meaningful frequency folding.

Motivated by graph total-variation based frequency analysis [35], the frequency associated with an eigenvalue  $\lambda[k]$  is determined by the number of the oscillations of the corresponding eigenvectors  $\mathcal{F}_k^{-1}$ , which is measured by its generalized total variation:

$$\|\nabla \mathcal{F}_k^{-1}\|_1 = \|(I - \mathcal{T}) \mathcal{F}_k^{-1}\|_1 = |1 - \lambda[k]| \cdot \|\mathcal{F}_k^{-1}\|_1.$$

Then, we consider the following ordering strategy of eigenvalues in terms of frequency magnitude, i.e.

$$\mathcal{F} \mathcal{T} \mathcal{F}^{-1} = \text{diag}(\lambda[1], \lambda[2], \dots, \lambda[N]),$$

382 such that the corresponding eigenvectors satisfy

$$383 \quad (4.5) \quad \|\nabla \mathcal{F}_1^{-1}\|_1 \leq \|\nabla \mathcal{F}_N^{-1}\|_1 \leq \|\nabla \mathcal{F}_2^{-1}\|_1 \leq \|\nabla \mathcal{F}_{N-1}^{-1}\|_1 \leq \dots \leq \|\nabla \mathcal{F}_{\frac{N}{2}}^{-1}\|_1 \leq \|\nabla \mathcal{F}_{\frac{N}{2}+1}^{-1}\|_1.$$

384 CONSTRUCTION 2. [Bandlimited down/up-sampling operator] Let  $\mathcal{F}$  denote the graph discrete  
 385 Fourier transform, whose columns follow the order (4.5). Recall that  $\mathcal{F} \in \mathbb{C}^{N \times N}$  is a unitary matrix.  
 386 Thus the matrix  $(I_{N/2}, I_{N/2}) \mathcal{F} \in \mathbb{C}^{\frac{N}{2} \times N}$  is of full row rank, and we form a matrix  $\bar{V} \in \mathbb{C}^{\frac{N}{2} \times \frac{N}{2}}$   
 387 whose columns contains  $N/2$  linearly independent columns of  $(I_{N/2}, I_{N/2}) \mathcal{F}$ . Consider the QR  
 388 decomposition of  $\bar{V}$ :

$$389 \quad (4.6) \quad \bar{V} = \bar{U} R,$$

390 where  $\bar{U} \in \mathbb{C}^{\frac{N}{2} \times \frac{N}{2}}$  is a unitary matrix and  $R \in \mathbb{C}^{\frac{N}{2} \times \frac{N}{2}}$  is an upper triangular matrix. Then, we  
 391 define the down-sampling and up-sampling operators,  $\Gamma_{\downarrow}$  and  $\Gamma_{\uparrow}$ , by

$$392 \quad (4.7) \quad \Gamma_{\downarrow} = \frac{1}{\sqrt{2}} (\bar{U}^*, \bar{U}^*) \mathcal{F} \quad \text{and} \quad \Gamma_{\uparrow} = \frac{1}{\sqrt{2}} \mathcal{F}^* \begin{pmatrix} \bar{U} \\ \bar{U} \end{pmatrix}.$$

Indeed, the down/up-sampling operator constructed in Construction 2 satisfies the condition imposed in Definition 4.4 by the fact that

$$\Gamma_{\downarrow} \Gamma_{\uparrow} = \frac{1}{2} (\bar{U}^*, \bar{U}^*) \mathcal{F} \mathcal{F}^* \begin{pmatrix} \bar{U} \\ \bar{U} \end{pmatrix} = \frac{1}{2} (\bar{U}^* U + \bar{U}^* U) = I_{N/2}.$$

393

394 PROPOSITION 4.7. Let  $\Gamma_\downarrow$  and  $\Gamma_\uparrow$  be the down-sampling and up-sampling operators defined in  
 395 Construction 2. Then  $\Gamma_\downarrow^* = \Gamma_\uparrow$  and  $\Gamma_\downarrow\Gamma_\uparrow$  is invertible.

396 A signal  $f \in \mathbb{C}^N$  defined on the graph  $G$  is called band-limited if its frequencies vanish outside  
 397 the half of the frequency domain:

$$398 \quad (4.8) \quad (\mathcal{F}f)[k] = 0, \quad \text{for } \frac{N}{2} - \lfloor \frac{N}{4} \rfloor + 1 \leq k \leq \frac{N}{2} + \lceil \frac{N}{4} \rceil.$$

399

400 PROPOSITION 4.8 (Band-limited down-sampling). Consider a band-limited signal  $f \in \mathbb{C}^N$  sat-  
 401 isfying (4.8) with even-length. Let  $\Gamma_\downarrow$  denote the down-sampling operator defined by (4.7). Then,  
 402  $f$  can be perfectly reconstructed from  $\Gamma_\downarrow f$ .

*Proof.* Consider a band-limited signal  $f \in \mathbb{C}^N$  satisfying (4.8). Note that

$$\Gamma_\downarrow f = \frac{1}{\sqrt{2}} \bar{U}^* (I, I) \mathcal{F}f = \frac{1}{\sqrt{2}} \bar{U}^* \begin{pmatrix} (\mathcal{F}f)[1] \\ (\mathcal{F}f)[2] \\ \vdots \\ (\mathcal{F}f)[\frac{N}{2} - \lfloor \frac{N}{4} \rfloor] \\ (\mathcal{F}f)[\frac{N}{2} + \lceil \frac{N}{4} \rceil + 1] \\ \vdots \\ (\mathcal{F}f)[N-1] \\ (\mathcal{F}f)[N] \end{pmatrix}.$$

Then  $f = \mathcal{F}^* \mathcal{F}f = \mathcal{F}^* x$ , where  $x \in \mathbb{C}^N$  is defined as

$$x[n] = \begin{cases} \sqrt{2}(\bar{U}\Gamma_\downarrow f)[n] & 1 \leq n \leq \frac{N}{2} - \lfloor \frac{N}{4} \rfloor \\ 0 & \frac{N}{2} - \lfloor \frac{N}{4} \rfloor + 1 \leq n \leq \frac{N}{2} + \lceil \frac{N}{4} \rceil \\ \sqrt{2}(\bar{U}\Gamma_\downarrow f)[n - \frac{N}{2}] & \frac{N}{2} + \lceil \frac{N}{4} \rceil + 1 \leq n \leq N \end{cases}.$$

403 Therefore,  $f$  can be perfectly reconstructed from  $\Gamma_\downarrow f$ . □

404 The basic operations introduced for signals on graph in this section are consistent with their  
 405 counterparts for signals on 1D equispaced Euclidean grid with periodic boundary extension. Consider  
 406 a finite signal  $f \in \mathbb{C}^N$  with periodic boundary extension. Then, the corresponding adjacency matrix  
 407 is given by

$$408 \quad S = \begin{pmatrix} 0 & 1 & & 1 \\ 1 & 0 & 1 & \\ & 1 & 0 & \\ & & & \ddots & 1 \\ 1 & & & 1 & 0 \end{pmatrix}.$$

Then the classic discrete Fourier transform  $\mathcal{F}$  defined by

$$\mathcal{F}[j, k] = N^{-\frac{1}{2}} e^{i2\pi \frac{(j-1)(k-1)}{N}}, \quad 1 \leq j, k \leq N.$$

will diagonalize the matrix  $S$

$$\mathcal{F}^{-1}S\mathcal{F} = 2 \cdot \text{diag}\left(1, \cos \frac{2\pi}{N}, \cos \frac{4\pi}{N}, \dots, \cos \frac{2(N-1)\pi}{N}\right).$$

By the construction scheme proposed in Construction 1 for the graph shift operator  $\mathcal{T}$ , we have

$$\mathcal{T} = \mathcal{F}^{-1}\left(\text{diag}\left(1, e^{\frac{i2\pi}{N}}, e^{\frac{i2\pi^2}{N}}, \dots, e^{\frac{i2\pi(N-1)}{N}}\right)\right)\mathcal{F},$$

409 whose matrix form is

$$410 \begin{pmatrix} 0 & & & 1 \\ 1 & 0 & & \\ & & \ddots & \\ & & & 1 & 0 \end{pmatrix}.$$

Thus,  $\mathcal{T}^k$  is exactly the  $k$ -tap shift operator:

$$\mathcal{T}^k : f[n] \rightarrow f[(n-k) \bmod N],$$

and the discrete convolution defined in Definition 4.2 is also the same as classic discrete convolution with periodic boundary extension:

$$(f \otimes h)[n] = \sum_{k \in \text{supp}(h)} h[k]f[(n-k) \bmod N].$$

411 For dyadic down-sampling operator, we have

$$412 \quad (4.9) \quad \Gamma_{\downarrow} = \begin{pmatrix} 1 & 0 & 0 & \cdots & 0 & 0 & 0 \\ 0 & 0 & 1 & \cdots & 0 & 0 & 0 \\ & & & \ddots & & & \\ 0 & 0 & 0 & \cdots & 1 & 0 & 0 \\ 0 & 0 & 0 & \cdots & 0 & 0 & 1 \end{pmatrix} \in \mathbb{C}^{\frac{N}{2} \times N}$$

413 and  $\Gamma_{\uparrow} = (\Gamma_{\downarrow})^*$ . It is also consistent with classic dyadic down-sampling and up-sampling operator  
414 for signals on equispaced grids.

415 **5. Multi-level framelet transform on graph.** After introducing the key building blocks for  
416 framelet transform on graph, we are ready to introduce multi-level framelet transform for signals  
417 on graph. Consider a signal  $f \in \mathbb{C}^N$  defined on a connected undirected graph  $G = \{\mathcal{V}, E, \omega\}$   
418 with adjacency matrix  $S$ . Let  $H = \{h_0, h_1, \dots, h_r\}$  and  $\tilde{H} = \{\tilde{h}_0, \tilde{h}_1, \dots, \tilde{h}_r\}$  denote the filter  
419 banks for framelet decomposition and reconstruction respectively. In parallel to framelet transform  
420 on equispaced grids, the undecimal framelet transform on graph is also built on decimal framelet  
421 transform by removing down-sampling operator at each level.

For a finite filter  $h$ , the transit operator  $W_h^d$  and the subdivision operator  $(W_h^d)^*$  are defined as

$$W_h^d = \Gamma_{\downarrow} \mathcal{H}(h^*(-\cdot)), \quad \text{and} \quad (W_h^d)^* = \mathcal{H}(h)\Gamma_{\uparrow},$$

422 where the convolution matrix  $\mathcal{H}(h)$  and down/up-sampling operators are defined as Definition 4.2  
423 and Definition 4.4. Then, the one-level decimial framelet transform is given by

$$424 \quad (5.1) \quad f \longrightarrow c := (W_{h_0}^d f; W_{h_1} f; \dots; W_{h_r}^d f) \quad (\text{decomoposition}),$$

425 and

$$426 \quad (5.2) \quad c \longrightarrow (W_{h_0}^d)^* c_0 + (W_{h_1}^d)^* c_1 + \dots + (W_{h_r}^d)^* c_r \quad (\text{reconstruction}).$$

427 It can be seen from that the one-level framelet transform depends on the shift operator  $\mathcal{T}$  de-  
428 rived from the underlying graph. The  $L$ -level framelet transform for signals on graph  $G$  has the  
429 same recursive scheme as the counterpart for equispaced Euclidean grids, i.e., the one-level discrete  
430 framelet transform is recursively applied on the output generated by a low-pass filter to generate a  
431 multi-level decomposition of input signal. The main difference between equi-spaced grid and general  
432 graph lies in the changes of the underlying structure after down-sampling. The underlying graph  
433 remains an equispaced grid after down-sampling the signal on a equispaced grid. Thus, the shift  
434 operator keep the same across different levels, up to grid size. In contrast, for a general graph, a  
435 meaningful down-sampling operator with good abstraction will change the underlying graph structure  
436 of downsampled signals. In other words, the shift operator varies at different levels, which leads to  
437 different one-level framelet transform at different level.

In the next, we propose a recursive scheme for defining the shift operators at different levels:

$$\mathcal{T}^{(1)}, \mathcal{T}^{(2)}, \dots, \mathcal{T}^{(L)},$$

438 for an undirected graph  $G$ .

439 CONSTRUCTION 3. Let  $\mathcal{T}^{(1)} = \mathcal{T}$  be the graph shift operator at the finest level given in Definition  
440 4.1, which is derived from the normalized adjacency matrix of the graph. Let  $\Gamma_{\downarrow}^{(1)} / \Gamma_{\uparrow}^{(1)}$  be the  
441 bandlimited down/up-sampling operator defined in Construction 2. The construction of the graph  
442 shift operator  $\mathcal{T}^{(2)}$  is then motivated by the observation on equispaced grids that shifting a down-  
443 sampled signal by 1-tap is closely related to down-sampling the original signal shifted by 2-tap.  
444 Notice that the band-limited down/up-sampling operator in Construction 2 has

$$445 \quad (5.3) \quad \Gamma_{\downarrow} \left( (\mathcal{T})^2 + (\mathcal{T}^*)^2 \right) \Gamma_{\uparrow} = \bar{U}^* \tilde{\Sigma} \bar{U},$$

446 where  $\bar{U} \in \mathbb{C}^{\frac{N}{2} \times \frac{N}{2}}$  is the unitary matrix defined from (4.6) and  $\tilde{\Sigma} \in \mathbb{C}^{\frac{N}{2} \times \frac{N}{2}}$  is a real-valued diagonal  
447 matrix. The shift operator  $\mathcal{T}^{(2)} \in \mathbb{C}^{\frac{N}{2} \times \frac{N}{2}}$  for the second level is then defined as a normal and  
448 invertible matrix that satisfies

$$449 \quad (5.4) \quad \mathcal{T}^{(2)} + \left( \mathcal{T}^{(2)} \right)^* = \bar{U}^* \tilde{\Sigma} \bar{U},$$

Since  $\bar{U}^* \tilde{\Sigma} \bar{U}$  is a Hermitian matrix, one can use Construction 1 to construct an isometric shift  
operator  $\mathcal{T}^{(2)}$ . The unitary matrix, denoted by  $\mathcal{F}^{(2)} \in \mathbb{C}^{\frac{N}{2} \times \frac{N}{2}}$ , that diagonalizes  $\mathcal{T}^{(2)}$  is defined  
as the Fourier transform at the second level. For example,  $\mathcal{F}^{(2)} = \bar{U}$  when  $\mathcal{T}^{(2)}$  is the defining  
isometric shift operator in Construction 1. By the same procedure, one can recursively define  
 $\mathcal{T}^{(3)}, \mathcal{T}^{(4)}, \dots, \mathcal{T}^{(L)}$ . By (5.3) and (5.4), we have

$$\mathcal{T}^{(\ell+1)} + \left( \mathcal{T}^{(\ell+1)} \right)^* = \Gamma_{\downarrow}^{(\ell)} \left( \left( \mathcal{T}^{(\ell)} \right)^2 + \left( \left( \mathcal{T}^{(\ell)} \right)^* \right)^2 \right) \Gamma_{\uparrow}^{(\ell)}, \quad \ell = 1, \dots, L-1.$$

450 It can be seen from the equation above that, shifting the signal by 1 tap in the coarser level is the same  
 451 as shifting the signal by 2 taps in the finer level, in which two levels are related via down-sampling  
 452 and up-sampling operations.

After defining the sequence of graph shift operators, for any filter  $h$ , we then have the definition of the convolution at the  $\ell$ -th level:

$$H^{(\ell)}(h) = \sum_{k \in \text{supp}(h)} h[k](\mathcal{T}^{(\ell)})^k.$$

453 Now, we have the following recursive procedure for an  $L$ -level decimal framelet transform on graph:

$$454 \quad (5.5) \quad \begin{aligned} \text{Decomposition : } & c_0^{(0)} := f, \quad c_j^{(\ell)} := W_{\tilde{h}_j}^{(\ell)} c_0^{(\ell-1)} \text{ for } 0 \leq j \leq r, 1 \leq \ell \leq L; \\ \text{Reconstruction : } & c_0^{(\ell)} := \sum_{j=0}^r (W_{\tilde{h}_j}^*)^{(\ell+1)} c_j^{(\ell+1)} \text{ for } \ell = L-1, \dots, 1, 0, \quad g := c_0^{(0)}, \end{aligned}$$

where

$$W_h^{(\ell)} = \Gamma_{\downarrow}^{(\ell)} H^{(\ell)}(h^*(\cdot)), \quad \text{and} \quad (W_{\tilde{h}}^*)^{(\ell)} = H^{(\ell)}(h) \Gamma_{\uparrow}^{(\ell)}.$$

455 In contrast to equispace grids, for general graphs, it is very difficult to have a filter bank with small  
 456 support, which can admit a decimal framelet transform with perfect reconstruction property. Taking  
 457 a single-level decimal framelet transform for example.

458 PROPOSITION 5.1. Let  $H = \{h_j\}_{j=0}^r$  and  $\tilde{H} = \{\tilde{h}_j\}_{j=0}^r$  be two sets of finite sequences supported  
 459 inside  $\mathbb{Z}_M$ . Then, the single-level discrete framelet transform defined by (5.5) with  $L = 1$  satisfies  
 460 the perfect reconstruction property if and only if  $H$  and  $\tilde{H}$  satisfy the following conditions:

$$461 \quad (5.6) \quad \begin{cases} \sum_{j=0}^r \sum_{k \in \mathbb{Z}_M} \sum_{p \in \mathbb{Z}_M+k} \tilde{h}_j[k] h_j^*[k-p] \lambda^p[m] = 2 \\ \sum_{j=0}^r \sum_{k \in \mathbb{Z}_M} \sum_{p \in \mathbb{Z}_M+k} \tilde{h}_j[k] h_j^*[k-p] \lambda_{\ell}^k[m] \lambda^{p-k}[(m + \frac{N}{2}) \bmod N] = 0, \end{cases} \quad \text{for } 1 \leq m \leq N.$$

462

*Proof.* The one-level framelet transform defined in (5.5) has perfect reconstruction property if and only if

$$\sum_{j=0}^r W_{\tilde{h}_j}^* W_{h_j} = I_N.$$

463 Notice that

$$464 \quad \begin{aligned} \sum_{j=0}^r W_{\tilde{h}_j}^* W_{h_j} &= \sum_{j=0}^r H(\tilde{h}_j) \Gamma_{\uparrow} \Gamma_{\downarrow} H(h_j^*(\cdot)) \\ &= \frac{1}{2} \sum_{j=0}^r H(\tilde{h}_j) \mathcal{F}^{-1} \begin{pmatrix} I_{\frac{N}{2}} & I_{\frac{N}{2}} \\ I_{\frac{N}{2}} & I_{\frac{N}{2}} \end{pmatrix} \mathcal{F} \mathcal{H}(h_j^*(\cdot)) \\ &= \frac{1}{2} \mathcal{F}^{-1} \left( \sum_{j=0}^r \sum_{k \in \mathbb{Z}_M} \sum_{p \in \mathbb{Z}_M+k} \tilde{h}_j[k] h_j^*[k-p] \Lambda^k \begin{pmatrix} I_{\frac{N}{2}} & I_{\frac{N}{2}} \\ I_{\frac{N}{2}} & I_{\frac{N}{2}} \end{pmatrix} \Lambda^{p-k} \right) \mathcal{F}. \end{aligned}$$

466

Therefore, the perfect reconstruction property holds if and only if

$$\sum_{j=0}^r \sum_{k \in \mathbb{Z}_M} \sum_{p \in \mathbb{Z}_M+k} \tilde{h}_j[k] h_j^*[k-p] \Lambda^k \begin{pmatrix} I_{\frac{N}{2}} & I_{\frac{N}{2}} \\ I_{\frac{N}{2}} & I_{\frac{N}{2}} \end{pmatrix} \Lambda^{p-k} = 2I_N,$$

467 which is equivalent to the following conditions, i.e. for any  $1 \leq m \leq N$ ,

$$\begin{aligned}
468 \quad & \sum_{j=0}^r \sum_{k \in \mathbb{Z}_M} \sum_{p \in \mathbb{Z}_{M+k}} \tilde{h}_j[k] h_j^*[k-p] \lambda^p[m] = 2, \\
469 \quad & \sum_{j=0}^r \sum_{k \in \mathbb{Z}_M} \sum_{p \in \mathbb{Z}_{M+k}} \tilde{h}_j[k] h_j^*[k-p] \lambda^k[m] \lambda^{p-k}[(m + \frac{N}{2}) \bmod N] = 0. \\
470 \quad &
\end{aligned}$$

471 This completes the proof.  $\square$

472 *It can be seen that in order to guarantee the perfect reconstruction property of a one-level*  
473 *framelet transform on a general graph, the two filter banks  $H$  and  $\tilde{H}$  need to satisfy totally  $N$*   
474 *bi-linear equations. As  $N$  is the number of vertices, the construction of such filter banks becomes*  
475 *increasingly difficult for the graph with large size.*

476 **REMARK 1.** *When the graph is bi-partite whose spectrum is symmetric about the zero, e.g. cycle*  
477 *graph with an even number of vertices, the condition (5.6) can be simplified to*

$$\begin{aligned}
478 \quad (5.7) \quad & \sum_{j=0}^r \sum_{k \in \mathbb{Z}_M} \sum_{p \in \mathbb{Z}_{M+k}} \tilde{h}_j[k] h_j^*[k-p] \lambda^p[m] = 2, \\
& \sum_{j=0}^r \sum_{k \in \mathbb{Z}_M} \sum_{p \in \mathbb{Z}_{M+k}} \tilde{h}_j[k] h_j^*[k-p] (-1)^{k-p} \lambda^p[m] = 0,
\end{aligned}$$

479 *which is exactly the UEP condition for classic framelet transform with perfect reconstruction prop-*  
480 *erty.*

481 *In the next, we present the undecimal discrete framelet transform which removes the down-*  
482 *sampling operation at each level. In parallel to the case of equispaced grid, the question is then what*  
483 *is the undecimal version of a down-sampled signal convolved with a filter, which is answered in the*  
484 *following proposition.*

**PROPOSITION 5.2.** *Let the operators  $\{\mathcal{T}^{(1)}, \mathcal{T}^{(2)}, \dots, \mathcal{T}^{(L)}\}$  denote the shift operators defined in*  
*Construction 3, which calls the construction schemes for shift operator and band-limited down/up*  
*sampling operator in Construction 1 and Construction 2. Let  $(\mathcal{T}^{(\ell)}, \Gamma_{\downarrow}^{(\ell)}, \Gamma_{\uparrow}^{(\ell)})$  denote the shift*  
*operator and down/up sampling operator for the  $\ell$ -th level. Then, there exists an invertible and*  
*normal matrix  $\mathcal{T}_u^{(\ell+1)} \in \mathbb{C}^{N \times N}$  such that*

$$\left( \mathcal{T}^{(\ell+1)} \right)^k \Gamma_{\downarrow}^{(\ell)} = \Gamma_{\downarrow}^{(\ell)} \left( \mathcal{T}_u^{(\ell+1)} \right)^k,$$

485 *for any  $k \in \mathbb{Z}$ .*

486 *Proof.* For the second level, let  $\mathcal{T}^{(2)}$  denote the shift operator defined via Construction 3.  
487 Let  $\Lambda^{(2)}$  denote the diagonal matrix associated with the eigenvalue decomposition of  $\mathcal{T}^{(2)}$ , i.e.  
488  $\mathcal{T}^{(2)} = \bar{U}^* \Lambda^{(2)} \bar{U}$ . Then  $\Lambda^{(2)}$  is invertible by the definition of  $\mathcal{T}^{(2)}$ . Define

$$489 \quad (5.8) \quad \mathcal{T}_u^{(2)} = (\mathcal{F}^{(1)})^* \begin{pmatrix} \Lambda^{(2)} & \\ & \Lambda^{(2)} \end{pmatrix} \mathcal{F}^{(1)},$$

where  $\mathcal{F}^{(1)}$  denotes graph Fourier transform of the previous level. Then, we have for any  $k \in \mathbb{Z}$ ,

$$\left( \mathcal{T}^{(2)} \right)^k \Gamma_{\downarrow} = \frac{1}{\sqrt{2}} \bar{U}^* \left( \Lambda^{(2)} \right)^k (I, I) \mathcal{F}^{(1)} = \Gamma_{\downarrow} \left( \mathcal{T}_u^{(2)} \right)^k.$$

Recursively applying the argument above, we have that

$$\left(\mathcal{T}^{(\ell+1)}\right)^k \Gamma_{\downarrow}^{(\ell)} = \Gamma_{\downarrow}^{(\ell)} \left(\mathcal{T}_u^{(\ell+1)}\right)^k, \quad k \in \mathbb{Z}$$

490 for  $\ell = 1, 2, \dots, L-1$ . □

It can be seen from the proposition above that the undecimal version of the shift operator  $\mathcal{T}^{(\ell)}$  at the  $\ell$ -th level is the shift operator denoted by  $\mathcal{T}_u^{(\ell)}$ , where  $\mathcal{T}_u^{(1)} = \mathcal{T}^{(1)}$ , and for  $\ell \geq 2$ ,  $\mathcal{T}_u^{(\ell)}$  can be recursively defined by the formula (5.8). Therefore, the convolution on a down-sampled signal can be expressed as down-sampling a signal after another convolution:

$$\mathcal{H}^{(\ell)}(h)\Gamma_{\downarrow}^{(\ell-1)} = \Gamma_{\downarrow}^{(\ell-1)}\mathcal{H}_u^{(\ell)}(h),$$

where the new convolution  $\mathcal{H}_u^{(\ell)}(h)$  is defined as

$$H_u^{(\ell)}(h) = \sum_{k \in \text{supp}(h)} h[k](\mathcal{T}_u^{(\ell)})^k.$$

Then, at the  $\ell$ -th level, the transit operator and the subdivision operator in the undecimal case is defined by

$$W_h^{(\ell)} : f \rightarrow \mathcal{H}_u^{(\ell)}(h(-\cdot)^*)f, \quad \text{and} \quad (W_h^*)^{(\ell)} : f \rightarrow \mathcal{H}_u^{(\ell)}(h)f.$$

491 Now, all operations involved in the framelet transform at the  $\ell$ -level are defined. For simplicity of  
 492 discussion, we assume that  $N$  can be divided by  $2^L$  for some positive integer  $L$ . See Algorithm 5.2  
 493 for the outline of the undecimal framelet transform for signals on graph.

---

**Algorithm 5.1**  $L$ -level undecimal framelet transform for signals on graph

---

- **Decomposition:**  $W_L : f \rightarrow c$ 
    - 1: **INPUT:** signal  $f$
    - 2: **OUTPUT:** framelet coefficients  $\{c_1^{(\ell)}, c_2^{(\ell)}, \dots, c_r^{(\ell)}\}_{\ell=1}^L \cup c_0^{(L)}$
    - 3: Set  $c_0^{(0)} = f$
    - 4: **for**  $\ell = 1, 2, \dots, L$  **do**
    - 5:      $c_j^{(\ell)} = W_{h_j}^{(\ell)} c_0^{(\ell-1)}$ , for  $0 \leq j \leq r$
    - 6: **end for**
  - **Reconstruction:**  $\widetilde{W}_L^* : c \rightarrow f$ 
    - 1: **INPUT:** framelet coefficients  $\{c_1^{(\ell)}, c_2^{(\ell)}, \dots, c_r^{(\ell)}\}_{\ell=1}^L \cup c_0^{(L)}$
    - 2: **OUTPUT:** signal  $f$
    - 3: **for**  $\ell = L-1, \dots, 1, 0$  **do**
    - 4:      $c_0^{(\ell)} = \sum_{j=0}^r (W_{\widetilde{h}_j}^*)^{(\ell+1)} c_j^{(\ell+1)}$  (bi-frames), or  $c_0^{(\ell)} = \sum_{j=0}^r (W_{h_j}^*)^{(\ell+1)} c_j^{(\ell+1)}$  (tight frame)
    - 5: **end for**
    - 6: Set  $f = c_0^{(0)}$
- 

494 In the next, we establish a sufficient condition on the two filter banks,  $H = \{h_0, h_1, \dots, h_r\}$   
 495 and  $\widetilde{H} = \{\widetilde{h}_0, \widetilde{h}_1, \dots, \widetilde{h}_r\}$ , that admits the perfect reconstruction property of multi-level undecimal

496 discrete framelet transform. Recall that the perfect reconstruction property refers to that the signal  
 497 can be exactly recovered using frame reconstruction operator from its framelet decomposition coeffi-  
 498 cients. The perfect reconstruction property of  $L$ -level discrete framelet transform will hold true, as  
 499 long as the one-level discrete framelet transform at each level has perfect reconstruction property,  
 500 i.e.

$$501 \quad (5.9) \quad (W_{\tilde{H}}^*)^{(\ell)} W_H^{(\ell)} = \sum_{j=0}^r (W_{\tilde{h}_j}^*)^{(\ell)} W_{h_j}^{(\ell)} = I_N,$$

502 for  $\ell = 1, 2, \dots, L$ .

503 **THEOREM 5.3** (Perfect reconstruction property for bi-framelet transform). Let  $H = \{h_j\}_{j=0}^r$   
 504 and  $\tilde{H} = \{\tilde{h}_j\}_{j=0}^r$  be two sets of finite sequences supported inside  $\mathbb{Z}_M$ . Then, the corresponding  $L$ -  
 505 level discrete undecimal framelet transform satisfies the perfect reconstruction property if  $H$  satisfies  
 506 the following conditions:

$$507 \quad (5.10) \quad \sum_{j=0}^r \sum_{k \in \mathbb{Z}_M} \tilde{h}_j[k] h_j^*[k-p] = \delta_p, \quad p \in \mathbb{Z}_N.$$

508 *Proof.* For the  $\ell$ -th level decomposition, it can be seen that

$$\begin{aligned} 509 \quad (W_{\tilde{H}}^*)^{(\ell)} W_H^{(\ell)} &= \sum_{j=0}^r (W_{\tilde{h}_j}^*)^{(\ell)} W_{h_j}^{(\ell)} \\ 510 &= \sum_{j=0}^r \sum_{k \in \mathbb{Z}_M} \sum_{p \in \mathbb{Z}_M+k} \tilde{h}_j[k] h_j^*[k-p] \left(\mathcal{T}_u^{(\ell)}\right)^k \left(\mathcal{T}_u^{(\ell)}\right)^{p-k} \\ 511 &= \sum_{j=0}^r \sum_{p \in \mathbb{Z}_{2M}} \sum_{k \in \mathbb{Z}_M \cap (\mathbb{Z}_M+p)} \tilde{h}_j[k] h_j^*[k-p] \left(\mathcal{T}_u^{(\ell)}\right)^k \left(\mathcal{T}_u^{(\ell)}\right)^{p-k} \\ 512 &= s_1 + s_2 + s_3, \end{aligned}$$

514 where

$$\begin{aligned} 515 \quad s_1 &= \sum_{j=0}^r \sum_{k \in \mathbb{Z}_M} \tilde{h}_j[k] h_j^*[k] \left(\mathcal{T}_u^{(\ell)} \left(\mathcal{T}_u^{(\ell)}\right)^{-1}\right)^k \\ 516 \quad s_2 &= \sum_{j=0}^r \sum_{p=-2M}^{-1} \sum_{k=-M}^{M+p} \tilde{h}_j[k] h_j^*[k-p] \left(\mathcal{T}_u^{(\ell)}\right)^p \\ 517 \quad s_3 &= \sum_{j=0}^r \sum_{p=1}^{2M} \sum_{k=-M+p}^M \tilde{h}_j[k] h_j^*[k-p] \left(\mathcal{T}_u^{(\ell)}\right)^p. \end{aligned}$$

519 Therefore, The perfect reconstruction property (5.9) is guaranteed if  $s_1 = I_N$  and  $s_2 = s_3 = 0$ ,

520 which leads to

$$\begin{aligned}
 521 \quad & \sum_{j=0}^r \sum_{k \in \mathbb{Z}_M} \tilde{h}_j[k] h_j^*[k] = 1, \\
 522 \quad & \sum_{j=0}^r \sum_{k=-M}^{p+M} \tilde{h}_j[k] h_j^*[k-p] = 0, \quad \forall p = -2M, \dots, -1, \\
 523 \quad & \sum_{j=0}^r \sum_{k=p-M}^M \tilde{h}_j[k] h_j^*[k-p] = 0, \quad \forall p = 1, \dots, 2M. \\
 524
 \end{aligned}$$

525 Therefore, the condition (5.9) holds true if

$$\begin{aligned}
 526 \quad & \sum_{j=0}^r \sum_{k \in \mathbb{Z}_M} \tilde{h}_j[k] h_j^*[k-p] = \delta_p, \quad \forall p \in \mathbb{Z}_N. \\
 527
 \end{aligned}$$

528 This completes the proof.  $\square$

529 *When using the same filter bank for both decomposition and reconstruction in tight framelet*  
 530 *transform, i.e.  $H = \tilde{H}$ , we have*

531 COROLLARY 5.4 (Perfect reconstruction property for tight framelet transform). *Let  $H =$*   
 532  *$\{h_j\}_{j=0}^r$  be one set of finite sequences supported inside  $\mathbb{Z}_M$ . Then, the corresponding  $L$ -level discrete*  
 533 *undecimal tight framelet transform satisfies the perfect reconstruction property if  $H$  satisfies the*  
 534 *following conditions:*

$$\begin{aligned}
 535 \quad (5.11) \quad & \sum_{j=0}^r \sum_{k \in \mathbb{Z}_M} h_j[k] h_j^*[k-p] = \delta_p, \quad p \in \mathbb{Z}_N.
 \end{aligned}$$

536 *The condition (5.11) indeed is one of the two conditions in (3.3) of the UEP for admitting*  
 537 *MRA-based wavelet tight frames for  $L^2(\mathbb{R})$ . In [30, 12], a class of spline wavelet tight frames with*  
 538 *arbitrary smoothness is constructed with explicit formulas for the associated filter banks, in which*  
 539 *the low-pass filters  $h_0$  are the refinement masks of B-splines with arbitrary degree.*

EXAMPLE 1 (B-spline filter banks [30, 12]). *The filter bank associated with linear B-spline*  
*tight frames is given by  $\tilde{H} = H$ , where*

$$H = \{h_0 = \frac{1}{4}[1, 2, 1], \quad h_1 = \frac{1}{4}[-1, 2, -1], \quad h_2 = \frac{\sqrt{2}}{4}[1, 0, -1]\}.$$

*The filter bank associated with Cubic B-spline tight frames is given by  $\tilde{H} = H = \{h_0, h_1, h_2, h_3, h_4\}$ ,*  
*where  $h_0 = \frac{1}{16}[1, 4, 6, 4, 1]$  and*

$$\begin{aligned}
 h_1 &= \frac{1}{16}[1, -4, 6, -4, 1], & h_2 &= \frac{1}{8}[-1, 2, 0 - 2, 1], \\
 h_3 &= \frac{\sqrt{6}}{16}[1, 0, -2, 0, 1], & h_4 &= \frac{1}{8}[-1, -2, 0, 2, 1].
 \end{aligned}$$

540 *We have both filter banks satisfy (5.11) and thus admit a multi-level undecimal framelet transform*  
 541 *with perfect reconstruction property.*

542 In the next, we give another sufficient condition on filter banks that admit tight framelet transforms  
 543 with perfect reconstruction property.

PROPOSITION 5.5. Consider a matrix  $H \in \mathbb{C}^{n \times (r+1)}$ . Let  $h_j$  denote the  $(j+1)$ -th column of  $H$  for  $0 \leq j \leq r$ . Suppose that  $H$  satisfies

$$HH^* = \frac{1}{\sqrt{n}}I_n.$$

544 Then, the filter bank  $\{h_0, h_1, \dots, h_r\}$  satisfies the condition (5.11).

*Proof.* By the condition

$$HH^* = \frac{1}{\sqrt{n}}I_n,$$

we have

$$\sum_{j=0}^r |h_j[k]|^2 = \frac{1}{\sqrt{n}} \quad \text{and} \quad \sum_{j=0}^r h_j[k]h_j^*[k'] = 0, \quad \forall k, k' \in \mathbb{Z}_M, k \neq k',$$

which leads to

$$\sum_{j=0}^r \sum_{k \in \mathbb{Z}_M} |h_j[k]|^2 = 1 \quad \text{and} \quad \sum_{j=0}^r \sum_{k \in \mathbb{Z}_M} h_j[k]h_j^*[k-p] = 0, \quad p \in \mathbb{Z}_N \setminus \{0\}.$$

545 Therefore, the condition (5.11) is satisfied. □

546 It can be seen from Proposition 5.5 that, as long as the filter bank forms a tight frame for  $\mathbb{C}^n$  (up to  
 547 a constant), we have a filter bank that admits a multi-level undecimal tight framelet transform with  
 548 perfect reconstruction property.

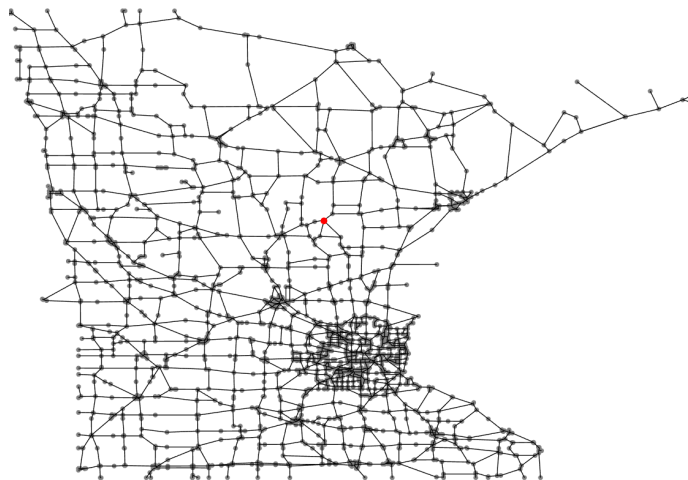


FIG. 5.1. Minnesota traffic graph

549 **6. Experiments and demonstrations.** *In this section, we demonstrate an example of discrete*  
 550 *framelet transform on irregular graph defined in previous sections, and run the transform on*  
 551 *some sample signals.*

552 **6.1. Scaling and Wavelet functions.** *Consider the graph shown in Figure 5.1 which de-*  
 553 *scribes the Minnesota transportation network where edges represent major roads, vertices represent*  
 554 *road intersections and edge weights are all equal to 1, i.e. the graph is unweighted. On such a graph,*  
 555 *we implement discrete framelet transform associated with the Haar filter bank  $H = \{\frac{1}{2}[1, 1], \frac{1}{2}[1, -1]\}$*   
 556 *and the linear B-spline filter bank  $H = \{\frac{1}{4}[1, 2, 1], \frac{1}{4}[-1, 2, -1], \frac{\sqrt{2}}{4}[1, 0, -1]\}$ . See Figure 6.1 and*  
 557 *Figure 7.1 for an illustration of scaling and wavelet functions (discrete) at different scales centered*  
 558 *at one vertex. It can be seen that, similar to its counterpart on equi-spaced grid, the scaling and*  
 559 *wavelet functions have good localization property in vertex domain, which indicates the desired ca-*  
 560 *pability of the resulting framelet transform on conducting local analysis of signals in vertex domain.*

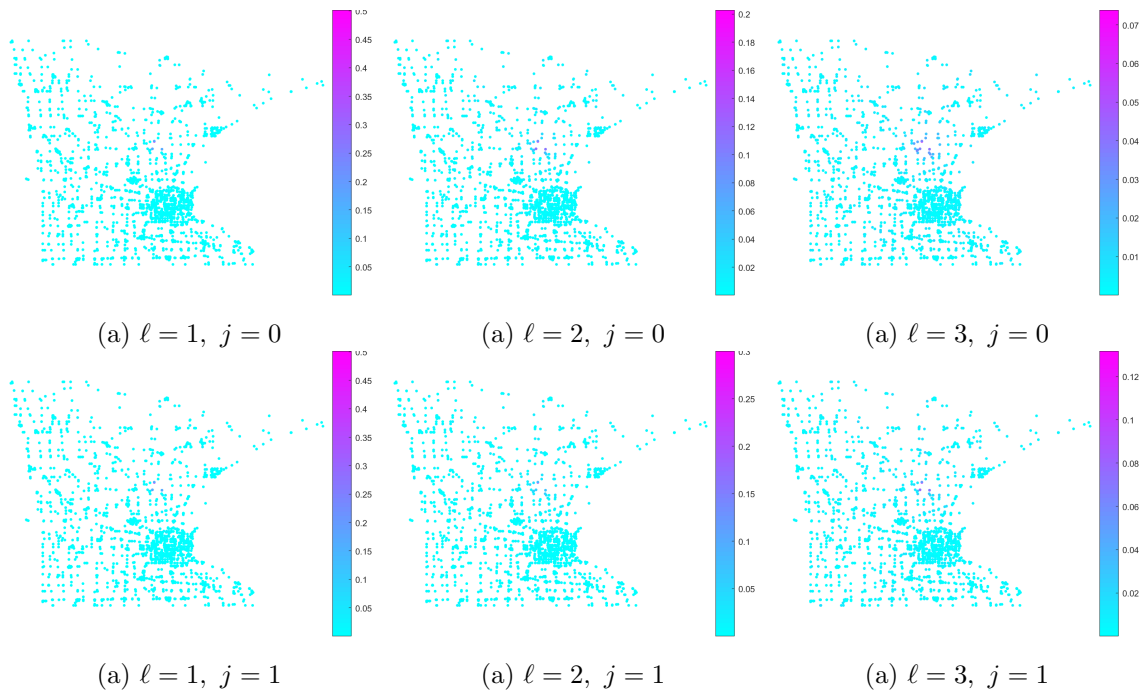


FIG. 6.1. Magnitude of scaling and wavelet functions centered at a vertex (red dot in Figure 5.1(a)), with respect to the haar filter bank  $H = \{\frac{1}{2}[1, 1], \frac{1}{2}[1, -1]\}$ .

561 **6.2. Sparse representation of framelet transform on graphs.** *Wavelet transform is*  
 562 *known for its efficiency on sparse approximation to piece-wise constant signals in Euclidean space.*  
 563 *Consider a piece-wise constant signal  $f$  defined on the Minnesota traffic graph shown in Figure 5.1,*  
 564 *which assigns two different values to a connected region and its complementary part in the graph. See*  
 565 *Figure 7.4 (a) for the visualization of such a graph structured signal. Two 3-level discrete framelet*  
 566 *transforms are applied on such a signal: one is based on the Haar filter bank and the other is*  
 567 *based on the linear B-spline filter bank. See Figure 7.2 and Figure 7.3 for the transform coefficients*

568 with respect to these two filter banks. It can be seen that in parallel to their counterparts on equi-  
 569 spaced grids, the high-pass framelet coefficients at different scales, e.g. the coefficients indexed at  
 570  $\ell = 1, 2, 3$  and  $j \neq 0$  are indeed sparse. See Figure 7.4 (b) for the histogram of high-pass framelet  
 571 coefficients. At last, we give an illustration on sparse approximation to piece-wise constant signal  
 572  $f$  shown in Figure 7.4 (a). The sparse approximation, denoted by  $\tilde{f}$ , is constructed by keeping low-  
 573 pass coefficients indexed at  $\ell = 3, j = 0$  and only 20% of all high-pass framelet coefficients indexed  
 574 at  $\ell = 1, 2, 3, j = 1, 2$ . The approximation error is  $\frac{\|f - \tilde{f}\|_2}{\|f\|_2} = 15.77\%$ . See Figure 7.4 (c) for the  
 575 visualization of  $\tilde{f}$ .

576 **7. Conclusion.** In this paper, we proposed a method to construct the multi-level undecimal  
 577 framelet transform for signals on undirected graph with perfect reconstruction property. By defining  
 578 basic blocks of framelet transform with strong motivation from its counterparts for equi-spaced grids,  
 579 including shift, convolution and up/down sampling, we have a painless construction scheme of  
 580 multi-level framelet transform whose associated filter bank can directly call those associated with  
 581 existing classic wavelet bi-frames and tight frames. The discrete framelet transform constructed  
 582 in this paper for graph keeps most desired properties of classic framelet transform, e.g., perfect  
 583 reconstruction property and efficient sparse approximation to piece-wise constant signals, which  
 584 makes it an appealing tool for processing and analyzing graph-structured signals.

585

## REFERENCES

- 586 [1] J. C. BREMER, R. R. COIFMAN, M. MAGGIONI, AND A. D. SZLAM, Diffusion wavelet packets, *Appl. Comput.*  
 587 *Harmon. Anal.*, 21 (2006), pp. 95–112.  
 588 [2] J.-F. CAI, R. CHAN, AND Z. SHEN, A framelet-based image inpainting algorithm, *Appl. Comput. Harmon.*  
 589 *Anal.*, 24 (2008), pp. 131–149.  
 590 [3] J.-F. CAI, H. JI, C. LIU, AND Z. SHEN, Framelet based blind image deblurring from a single image, *IEEE*  
 591 *Trans. Image Proc.*, 21 (2012), pp. 562–572.  
 592 [4] J.-F. CAI, H. JI, Z. SHEN, AND G. B. YE, Data-driven tight frame construction and image denoising, *Appl.*  
 593 *Comput. Harmon. Anal.*, 37 (2014), pp. 89–105.  
 594 [5] C. CHUI, F. FILBIR, AND H. MHASKAR, Representation of functions on big data: graphs and trees, *Appl.*  
 595 *Comput. Harmon. Anal.*, 38 (2015), pp. 489–509.  
 596 [6] C. K. CHUI, H. MHASKAR, AND X. ZHUANG, Representation of functions on big data associated with directed  
 597 graphs, *Appl. Comput. Harmon. Anal.*, 44 (2018), pp. 165–188.  
 598 [7] F. R. CHUNG, Spectral graph theory, vol. 92, *American Mathematical Soc.*, 1997.  
 599 [8] R. COIFMAN AND D. DONOHO, Translation-invariant de-noising, in *Wavelet and Statistics*, vol. 103 of *Springer*  
 600 *Lecture Notes in Statistics*, Springer-Verlag., 1994, pp. 125–150.  
 601 [9] R. R. COIFMAN AND M. MAGGIONI, Diffusion wavelets, *Appl. Comput. Harmon. Anal.*, 21 (2006), pp. 53–94.  
 602 [10] M. CROVELLA AND E. KOLACZYK, Graph wavelets for spatial traffic analysis, in *Proc. of INFOCOM*, vol. 3,  
 603 *IEEE*, 2003, pp. 1848–1857.  
 604 [11] I. DAUBECHIES, Ten lectures on wavelets, vol. 61, *SIAM*, 1992.  
 605 [12] I. DAUBECHIES, B. HAN, A. RON, AND Z. SHEN, Framelets: MRA-based constructions of wavelet frames, *Appl.*  
 606 *Comput. Harmon. Anal.*, 14 (2003), pp. 1–46.  
 607 [13] B. DONG, Sparse representation on graphs by tight wavelet frames and applications, *Appl. Comput. Harmon.*  
 608 *Anal.*, 42 (2017), pp. 452–479.  
 609 [14] B. DONG AND Z. SHEN, Mra-based wavelet frames and applications, in *IAS/Park City Mathematics Series:*  
 610 *The Mathematics of Image Processing*, vol. 19, 2010, pp. 7–185.  
 611 [15] Z. FAN, A. HEINECKE, , AND Z. SHEN, Duality for frames, *J. Fourier Anal. Appl.*, (2015).  
 612 [16] M. GAVISH, B. NADLER, AND R. R. COIFMAN, Multiscale wavelets on trees, graphs and high dimensional data:  
 613 Theory and applications to semi supervised learning, in *ICML*, 2010, pp. 367–374.  
 614 [17] D. K. HAMMOND, P. VANDERGHEYNST, AND R. GRIBONVAL, Wavelets on graphs via spectral graph theory,  
 615 *Appl. Comput. Harmon. Anal.*, 30 (2011), pp. 129–150.  
 616 [18] N. LEONARDI AND D. VAN DE VILLE, Wavelet frames on graphs defined by fmri functional connectivity, in  
 617 *ISBI*, *IEEE*, 2011, pp. 2136–2139.

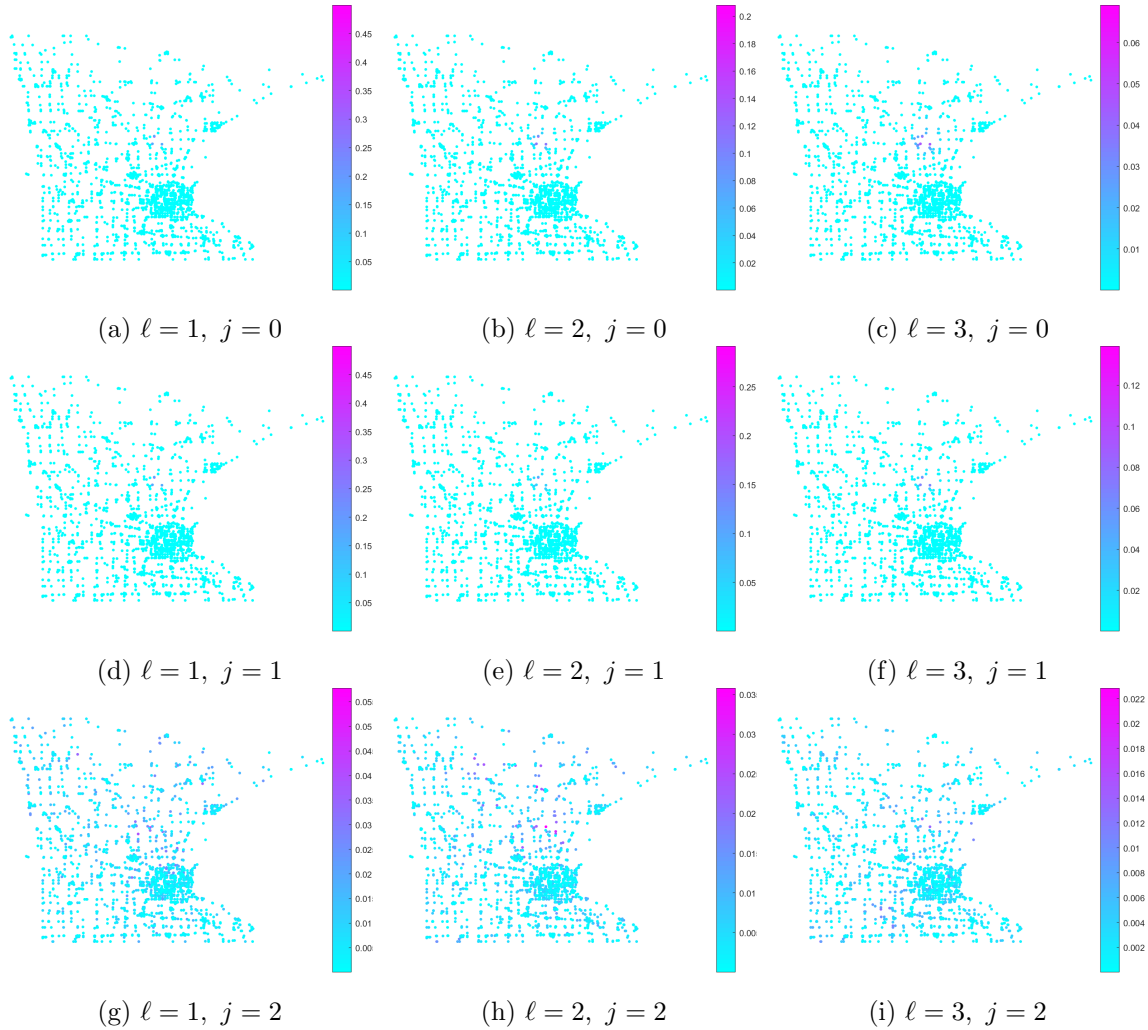


FIG. 7.1. The magnitude of scaling function and wavelet functions centered at one vertex (red dot in Figure 5.1(a)), with respect to the filter bank  $H = \{\frac{1}{4}[1, 2, 1], \frac{1}{4}[-1, 2, -1], \frac{\sqrt{2}}{4}[1, 0, -1]\}$ .

- 618 [19] N. LEONARDI AND D. V. D. VILLE, Tight wavelet frames on multislice graphs, *IEEE Trans. Signal Process.*,  
 619 61 (2013), pp. 3357–3367.
- 620 [20] M. LI, Z. FAN, H. JI, AND Z. SHEN, Wavelet frame based algorithm for 3d reconstruction in electron microscopy,  
 621 *SIAM J. Sci. Comput.*, 36 (2014), pp. 45–69.
- 622 [21] M. MAGGIONI, J. C. BREMER, R. R. COIFMAN, AND A. D. SZLAM, Biorthogonal diffusion wavelets for multiscale  
 623 representations on manifolds and graphs, in *Wavelets XI*, vol. 5914, *International Society for Optics and*  
 624 *Photonics*, 2005, p. 59141M.
- 625 [22] S. MALLAT, A Wavelet Tour of Signal Processing, Third Edition: The Sparse Way, *Academic Press, San Diego,*  
 626 *CA*, 2008.
- 627 [23] S. K. NARANG AND A. ORTEGA, Lifting based wavelet transforms on graphs, in *APSIPA ASC, 2009*, pp. 441–  
 628 444.
- 629 [24] S. K. NARANG AND A. ORTEGA, Perfect reconstruction two-channel wavelet filter banks for graph structured

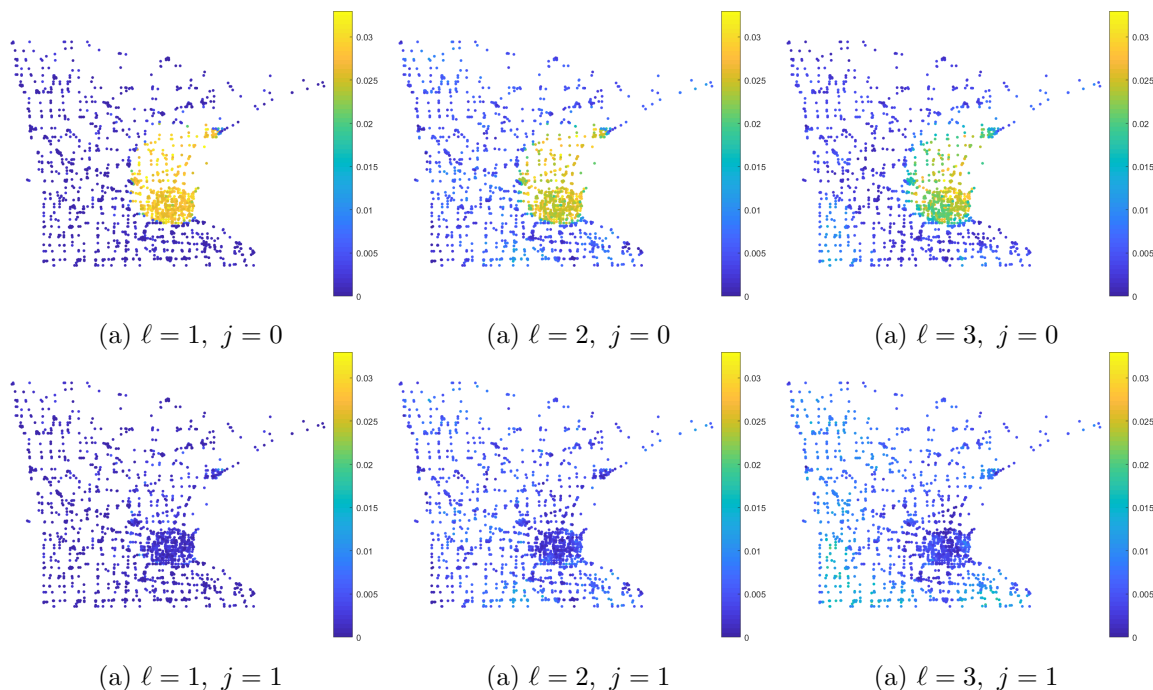


FIG. 7.2. The magnitude of framelet coefficients of piece-wise constant signals shown in Figure 5.1 (b), with respect to the Haar filter bank  $H = \{\frac{1}{2}[1, 1], \frac{1}{2}[1, -1]\}$ .

- 630 data, *IEEE Trans. Signal Process.*, 60 (2012), pp. 2786–2799.
- 631 [25] J. D. POWER, A. L. COHEN, S. M. NELSON, G. S. WIG, K. A. BARNES, J. A. CHURCH, A. C. VOGEL, T. O.  
 632 LAUMANN, F. M. MIEZIN, B. L. SCHLAGGAR, ET AL., Functional network organization of the human brain,  
 633 *Neuron*, 72 (2011), pp. 665–678.
- 634 [26] I. RAM, M. ELAD, AND I. COHEN, Generalized tree-based wavelet transform, *IEEE Trans. Signal Process.*, 59  
 635 (2011), pp. 4199–4209.
- 636 [27] I. RAM, M. ELAD, AND I. COHEN, Generalized tree-based wavelet transform, *IEEE Trans. Signal Process.*, 59  
 637 (2011), pp. 4199–4209.
- 638 [28] I. RAM, M. ELAD, AND I. COHEN, Redundant wavelets on graphs and high dimensional data clouds, *IEEE*  
 639 *Signal Process. Lett.*, 19 (2012), pp. 291–294.
- 640 [29] A. RON AND Z. SHEN, Affine system in  $L_2(\mathbb{R}^d)$ : the analysis of the analysis operator, *J. Funct. Anal.*, 148  
 641 (1997).
- 642 [30] A. RON AND Z. SHEN, Affine systems in  $L_2(\mathbb{R}^d)$  ii: Dual systems, *J. Fourier Anal. Appl.*, 3 (1997), pp. 617–637.
- 643 [31] A. SAKIYAMA, K. WATANABE, Y. TANAKA, AND A. ORTEGA, Two-channel critically sampled graph filter banks  
 644 with spectral domain sampling, *IEEE Trans. Signal Process.*, 67 (2019), pp. 1447–1460.
- 645 [32] A. SANDRYHAILA AND J. M. MOURA, Discrete signal processing on graphs, *IEEE Trans. Signal Process.*, 61  
 646 (2013), pp. 1644–1656.
- 647 [33] A. SANDRYHAILA AND J. M. MOURA, Discrete signal processing on graphs: Graph fourier transform., in  
 648 *ICASSP, 2013*, pp. 6167–6170.
- 649 [34] A. SANDRYHAILA AND J. M. MOURA, Big Data Analysis with Signal Processing on Graphs: Representation and  
 650 processing of massive data sets with irregular structure, *IEEE Signal Process. Mag.*, 31 (2014), pp. 80–90.
- 651 [35] A. SANDRYHAILA AND J. M. MOURA, Discrete signal processing on graphs: Frequency analysis., *IEEE Trans.*  
 652 *Signal Process.*, 62 (2014), pp. 3042–3054.
- 653 [36] G. SHEN AND A. ORTEGA, Optimized distributed 2d transforms for irregularly sampled sensor network grids  
 654 using wavelet lifting, in *ICASSP, IEEE, 2008*, pp. 2513–2516.

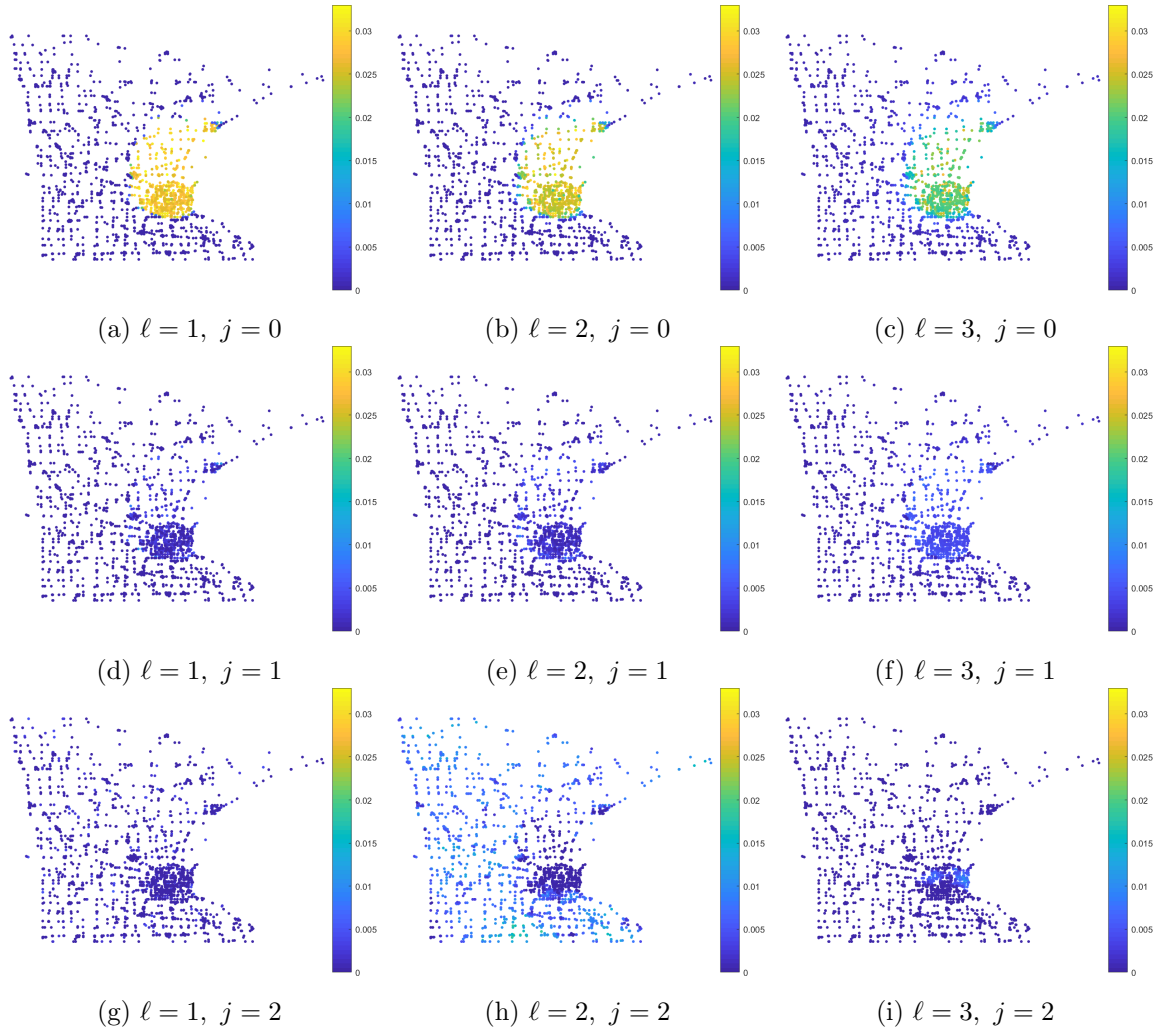


FIG. 7.3. The magnitude of framelet coefficients of the piece-wise constant signal shown in Figure 5.1 (b), with respect to the linear B-spline filter bank  $H = \{\frac{1}{4}[1, 2, 1], \frac{1}{4}[-1, 2, -1], \frac{\sqrt{2}}{4}[1, 0, -1]\}$ .

- 655 [37] G. SHEN AND A. ORTEGA, Transform-based distributed data gathering, *IEEE Trans. Signal Process.*, 58 (2010),  
 656 pp. 3802–3815.  
 657 [38] Z. SHEN, Wavelet frames and image restorations, in *Proc. ICM, vol. 4, Hindustan Book Agency, India, 2010*,  
 658 pp. 2834–2863.  
 659 [39] D. I. SHUMAN, C. EIESMEYR, N. HOLIGHAUS, AND P. VANDERGHEYNST, Spectrum-adapted tight graph wavelet  
 660 and vertex-frequency frames, *IEEE Trans. Signal Process.*, 63 (2015), pp. 4223–4235.

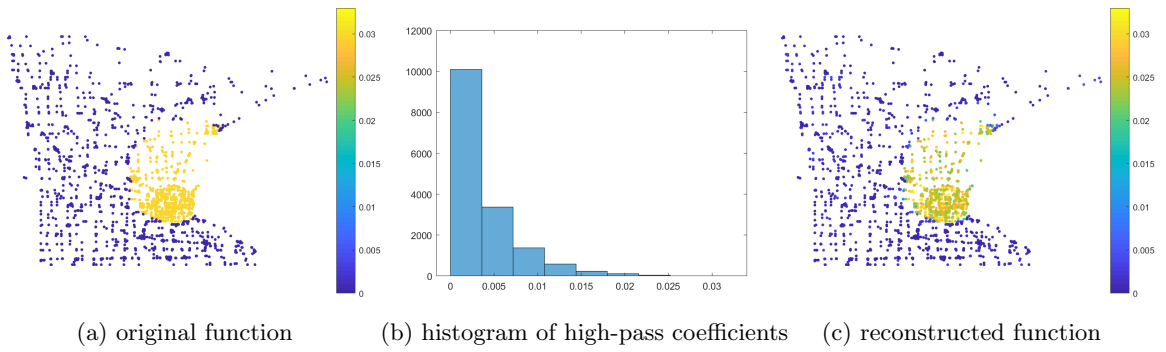


FIG. 7.4. The piece-wise constant function defined on the graph, and the reconstruction using partial coefficients of 3-level framelet transform associated with linear spline filter bank  $H = \{\frac{1}{4}[1, 2, 1], \frac{1}{4}[-1, 2, -1], \frac{\sqrt{2}}{4}[1, 0, -1]\}$  and level  $L = 3$ . The coefficients used for reconstruction include all low-pass coefficients and top 20% (in magnitude) high-pass coefficients.